Project THEMIS
Technical Report No. 17

WIND-TUNNEL MODELING OF FLOW AND DIFFUSION OVER AN URBAN COMPLEX

by

F. H. Chaudhry

and

J. E. Cermak

Prepared under

Office of Naval Research

Contract No. N00014-68-A-0493-0001

Project No. NR 062-414/6-6-68(Code 438)

U. S. Department of Defense

Washington, D.C.

Fluid Dynamics and Diffusion Laboratory
College of Engineering
Colorado State University
Fort Collins, Colorado

May, 1971

CER70-71FHC-JEC24

DISCLAIMER

THE FINDINGS IN THIS DOCUMENT ARE NOT TO BE CONSTRUED AS AN OFFICIAL DEPARTMENT OF THE ARMY POSITION UNLESS SO DESIGNATED BY OTHER AUTHORIZED DOCUMENTS. THE USE OF TRADE NAMES IN THIS REPORT DOES NOT CONSTITUTE AN OFFICIAL ENDORSEMENT OR APPROVAL OF THE USE OF SUCH COMMERCIAL HARDWARE OR SOFTWARE. THIS REPORT MAY NOT BE CITED FOR PURPOSES OF ADVERTISEMENT.

DISPOSITION INSTRUCTIONS

DESTROY THIS REPORT WHEN NO LONGER NEEDED
DO NOT RETURN IT TO THE ORIGINATOR

ABSTRACT

The purpose of this study is to explore and test the powerful potential of wind-tunnel modeling as an alternative to the more expensive and tedious full-scale urban diffusion experiments.

A model of the city of Fort Wayne was constructed to a horizontal scale of 1:4000 and a vertical scale of 1:2000. Flow and diffusion over the model was studied in the environmental wind tunnel of the Fluid Dynamics and Diffusion Laboratory at Colorado State University. If the roughness and the heat-island effects modeled properly, and the approach flows made similar, the flow over the model city was found to conform to that in the field. The pattern of the heat island over Fort Wayne is reproduced almost exactly in the model. Simulation of diffusion from an aerial line source was accomplished by traversing a continuously emitting source of Krypton-85 upwind of the city. The measured dosages of this tracer over the city compare well with the corresponding field data except immediately downwind from the source where the downdraft from the disseminating aircraft becomes significant in the field. The model is found to give same overall picture of the effect of the city on dispersion process as that observed in the field. The results show that the heat island effect vitiates the environment by bringing pollutants down from elevated releases through enhanced vertical mixing. The model results compare reasonably with approximate theory of Smith (1957).

The results of this study have proved that it is indeed possible to simulate the flow over a city and obtain useful information, relatively inexpensively, on urban diffusion. This investigation opens the way for studies of air-pollution problems for purposes of urban planning. The

location of industrial sites relative to major topographical features, the location of freeways through existing cities, the grouping of tall buildings in an urban-development program, or even the judicious placing of parks, residential and industrial areas in an entirely new city to minimize air pollution potentials under adverse meteorological conditions can be studied systematically.

ACKNOWLEDGMENT

This study was initiated by Deseret Test Center (Dugway Proving Ground) as an attempt to determine the feasibility of wind tunnel modeling of the meteorological regimes of cities as an alternative to making extensive field measurements. A copy of the original field study at Fort Wayne, Indiana by Hilst and Bowne (sponsored by Deseret Test Center through program 1T062111A128) was provided to Colorado State University by Deseret Test Center for comparative purposes and is normally available only in the Department of Defense. Funding for the wind tunnel study was provided by program 1T062111A128 through contract DAAB07-68-C-0423, which is monitored by the United States Army Electronics Command (ECOM) and administered by the United States Army Materiel Command (AMC).

The authors wish to acknowledge the help of all the personnel of the Fluid Mechanics Program, College of Engineering, Colorado State University, who were associated with this study.

Special thanks are due to Dr. G. Hsi for his contributions at the early stages of this work when the problems appeared insurmountable. The efforts of Mr. R. Johansen contributed greatly to the model construction. Our discussions with Messers J. Garrison, Fluid Dynamics Laboratory Supervisor and R. Asmus, Machine Shop Supervisor during design of equipment contributed very much toward performing the quasi-instantaneous diffusion experiments and are greatly appreciated.

Appreciation is expressed to Mr. S. Sethuraman and Mr. K. Nambudripad for their assistance in data collection and analysis. The writers are thankful to Dr. M. Julliand for his participation in the diffusion

experiments. Thanks are due to Miss H. Akari for excellent drafting and to Mary Grace Smith for careful typing.

LIST OF TABLES

LIST OF FIGURES

LIST OF FIGURES - (cont'd)

Figure | Page

LIST OF SYMBOLS

Symbol	Description
A	Area of the heated part of the model
c_f'	Local skin-friction coefficient
D	Dosage (μci-min/cc)
D_o	Non-dimensional ground level dosage
$\mathbb{D}$	Non-dimensional dosage = $\frac{Du_h h}{Q}$
g	Acceleration due to gravity
G	Geometrical factor in radiant heat-transfer
h	Source height
h_c	Convective heat-transfer Coefficient
k	Thermal conductivity
k_1	Actual height of roughness
k_s	Equivalent sand-roughness
K_h	Turbulent eddy diffusivity at height h
K_m	Turbulent eddy diffusivity for momentum
K_x	Turbulent eddy diffusivity in x - direction
K_z	Turbulent eddy diffusivity in z - direction
L	Characteristic length
m	Coefficient of relative surface rugosity
M	Subscript indicating a quantity pertaining to model
n	Number of nichrome wires in a circuit
p	Subscript indicating a quantity pertaining to prototype
P_r	Prandtl number = $\frac{\nu}{k/\rho c_p}$
q	Total heat transfer from the model
q_1	Convective heat transfer

LIST OF SYMBOLS - (cont'd)

Symbols	Description
q_2	Conductive heat transfer
q_3	Radiative heat transfer
R_{iB}	Bulk Richardson number = $\frac{gL\Delta T_o}{U_o^2 T_a}$
R_x	Reynolds number = $\frac{U_\infty x}{\nu}$
T	Temperature
T_a	Average temperature
T_f	Film temperature
T_∞	Free stream temperature
T'	Absolute temperature in degrees Rankine
ΔT_o	Temperature difference between the surface and reference height
u	Average velocity at any point
u_*	Shear velocity = $\sqrt{\tau_o/\rho}$
$\sqrt{\overline{u'^2}}$	R.M.S. of the fluctuating component of velocity
U	Average velocity at any point
U_o	Average velocity at the reference height
U_h	Average velocity at the height of source
U_∞	Free stream velocity
x,y,z	Distances in longitudinal, lateral and vertical directions
α	Exponant in power-law for velocity; also the vertical exaggeration of the model
γ	Concentration of roughness elements
ϵ	Emissivity
ζ	Non-dimensional height = $\frac{z}{h}$
ν	Kinematic viscosity
ξ	Non-dimensional longitudinal distance = $\frac{x K_h}{U_h h^2}$
ρ	Mean mass density of air

Symbol	Description
σ	Stefan-Boltzman constant
σ_z	Vertical dispersion
τ_o	Surface shear stress

TABLE OF CONTENTS

I. INTRODUCTION

Knowledge of turbulent diffusion over urban areas can be useful in predicting the occurrence of air-pollution episodes and controlling the release of pollutants into the atmosphere from existing or proposed industrial locations and thus improve the deteriorating urban atmosphere. The ability of the atmosphere to disperse the pollutants is variable especially in urban areas. Atmospheric dispersion processes are not completely predictable but the advances made in the last two decades enable one to estimate, with fair confidence, the concentrations of pollutants released over relatively flat terrain under different stability conditions. Diffusion over urban areas is more complex and involves additional parameters such as non-uniform surface roughness, topographic relief and climatic modifications due to higher temperatures in the city or the so called "heat-island effect".

Davis (1968) and Myrup (1969) have reviewed the urban heat-island studies and also the explanations for this phenomenon offered by different authors. The heat-island effect is associated in varying degrees with self heating due to industrial and domestic combustion in a city, crowded population, blanketing effect of urban atmospheric pollution, reduced evaporation, large heat capacity and conductivity of building and paving materials etc. Myrup (1969) concludes that the urban heat island is the result of a complex set of interacting physical processes. The urban heat-island effect is significant during inversion conditions in that it produces less stable lapse rates near the surface causing greater dispersion over urban areas.

Experimental investigations have formed the foundation of present understanding and practice of relating dispersion to meteorological

parameters in the atmosphere. The emphasis, however, has been on the study of diffusion over level terrain so that the problem of treating diffusion over complex surfaces is relatively new.

The experimental investigations of diffusion over urban areas are few and the results are inconclusive. Turner (1964) attempted to extend the Gaussian distribution approach to dispersion from multiple sources in Nashville, Tennessee for which 24-hr sulphur-dioxide measurements were made over a year. Seventy percent of the calculated values were found to be within a factor of two. This model, however, disregarded the topographic variations and heat-island effect in addition to other simplifying assumptions. Such attempts, while providing means of estimating pollution do not contribute toward understanding of the dispersion process. Pooler (1966) has reported a field program of a tracer study over St. Louis to obtain "evidence to indicate at least order-of-magnitude urban area dispersion parameter". The limited results suggested the formation of a slightly unstable layer as the air passed over the city during evening. The most exaustive field experiments, yet, are those performed at Fort Wayne, Indiana (Hilst and Bowne, 1966) to study primarily the influence of urban complex on atmospheric diffusion. In these experiments, diffusion downwind from a quasi-instantaneous line source created by release of flourescent pigment by an aeroplane flying cross wind was studied. A rather complete surface dosage distribution pattern in the city and the adjoining rural area were obtained. Their analysis revealed no preferred regions of high or low dosage within either city or rural areas. Hilst and Bowne (1966) concluded that a city of the size and structure of Fort Wayne may be considered a single surface anomaly for the purpose of predicting its effect on aerosol diffusion. Although this study provided a

set of data which is the best as yet, it has by no means completed the knowledge on urban effects. Many more experimental investigations need to be made; however, only a limited number is feasible due to the prohibitive cost of field studies. An alternative method is, therefore, required to inquire into this important problem.

Aerodynamic modeling has contributed greatly in the understanding of fluid-flow phenomena which cannot be treated theoretically or, experimentally through prototype investigations. The problem under consideration is defiant in the same manner and a logical approach to obtain further knowledge would be to make a scale-model study of dispersion over a typical city. Fort Wayne, Indiana is most suited for such a study for two reasons. Firstly, it has nearly all the characteristics of a typical big city with an environment made up of an industrial and agricultural complex and has the simplifying features of a surrounding flat rural topography. Secondly, extensive prototype data are available which can facilitate modeling the flow over the city. An attempt to study temperature distributions by modeling the urban atmosphere was made by Davis (1968). The basis of modeling and the interpretation of results by Davis left much to be desired in modeling of such flows. It is necessary to use the more accepted modeling techniques such as those discussed by Cermak et.al. (1965) and McVehil et.al. (1967). Although sufficient knowledge is available on wind-tunnel modeling to make studies of the urban atmosphere feasible, the correspondance between model and prototype result must, however, be established.

The purpose of this study is to explore and test the application of wind-tunnel modeling to diffusion over urban areas. If the model and prototype data compare favorably, this investigation would not only meet

the above stated objective but also open the way for studies of air pollution problems for purposes of urban planning. The location of industrial sites relative to major topographical features, the location of freeways through existing cities, the grouping of tall buildings in an urban development program, or even the geometrical features of an entirely new city to minimize air pollution potentials under adverse meteorological conditions could be studied systematically.

The experiments were performed in the new environmental wind tunnel of the Fluid Dynamics and Diffusion Laboratory at Colorado State University. The model of the city of Fort Wayne was constructed to a scale of 1:4000 in the horizontal and two main features which significantly effect atmospheric motion and aerosol dispersion have been incorporated into the model. One is the surface roughness in the form of buildings and the other is the "heat-island effect". The latter was accomplished by placing nichrome wires over the city area and applying a predetermined voltage.

A traversing system carrying a continuously emitting source of Krypton-85 upwind of the city to simulate aircraft releases of fluorescent particle tracers in the field. The modeling requirements, the experimental methods and the results are discussed in the following sections.

II. EXPERIMENTAL EQUIPMENT

2.1 Wind Tunnel

The experimental work was carried out in the new environmental wind tunnel of the Fluid Dynamics and Diffusion Laboratory at Colorado State University. Its large 12 ft wide test section can accommodate large models like that of the city of Fort Wayne. The environmental wind tunnel is an open-circuit type as shown in Fig. 1. A 150 H.P. blower generates stable air speeds from about 8 ft/sec up to 60 ft/sec in a 12 ft x 8 ft test section. The air speed is set by varying the fan-blade pitch. The wind-tunnel ceiling can be adjusted to achieve a zero pressure gradient in the longitudinal direction. The large entrance is provided with honey-comb straighteners and a pair of screens to calm the flow into the test section and eliminate large-scale disturbances.

A sizable portion of 52 ft long test section has a uniform free-stream velocity. Figure 2 shows the free-stream velocity variation. The pressure gradient along the tunnel was zero for this set of measurements. The effect of the constriction at the end of the wind tunnel extends upstream for about 12 ft only. The section of the wind tunnel between $x = 20$ ft and $x = 32$ ft, thus, seemed the most suitable one for the location of the model. Transverse velocity distributions at three different heights are shown in Fig. 3 for a free stream velocity of 10 ft/sec. These distributions are uniform and thus facilitate modeling of the approaching atmospheric flow which is a turbulent two-dimensional shear flow. The side-wall boundary layers are each about 10 in. thick, thus leaving a working width for the wind tunnel of more than 10 ft.

The velocity profiles exhibit a 1/7th power law behavior which is typical of turbulent boundary layers over flat terrain. The wind profiles

approaching the Fort Wayne model were, however, modified to match the field profiles. The modification technique is described later in this chapter.

2.2 Instrumentation and Measurement Techniques

2.2.1 Velocity profiles - The velocity distributions were measured with a pitot-static tube of standard design, 3.2 mm in diameter. The two pressure ports of the tube were connected to the two ports of an electronic differential pressure transducer (transonic, equibar tube 120). The pitot tube was mounted on a remote control vertical carriage and its vertical position was monitored through a potentiometer mounted on the carriage. The D.C. output of this differential-capacitor device was recorded on an x-y plotter versus the height of the pitot tube. Dynamic pressure profiles were converted to wind velocity by evaluating local density from local temperature and barometric-pressure measurements.

2.2.2 Temperature measurement - Surface air temperatures and temperature profiles in the thermal boundary layer were measured with copper-constantan thermocouples with their reference junctions in an ice bath. Fifty thermocouples were fixed on the surface of the model to obtain the spatial variation of temperature. The vertical profiles were taken by traversing a copper-constantan thermocouple on a carriage by remote control. The thermocouple emf was read out on a sensitive millivolt potentiometer.

2.2.3 Turbulence intensity profiles - Longitudinal turbulence intensity $(\frac{\sqrt{u'^2}}{U})$ profiles were measured by the use of a hot-wire probe mounted normally to the flow. The hot-wire sensor used in these experiments was 0.00035 in. diameter tungsten wire mounted on a Disa probe. A constant temperature hot-wire anemometer (FDDL-IL WW-WC-769-3) designed

at Colorado State University was used. The mean value of the anemometer output was measured by an integrator in conjunction with a Hewlett-Packard digital voltmeter. For the rms of the fluctuating signal a Disa Type 55 D 35 RMS voltmeter was used. In the thermally stratified flow, a hot-wire sensor responds to both the temperature and velocity fluctuations and measurement techniques are more involved. In the present study, the method developed by Corrsin (1949) and Kovasnay (1953) was used.

2.2.4 Visualization - Smoke was used to visually observe the diffusion patterns over the model. Titanium tetrachloride was used to provide dense smoke required for photographic purposes. A polaroid camera was used to photograph the plumes.

2.2.5 Diffusion tracer - Krypton-85 was used as a diffusion tracer for this investigation. It is a beta-emitting radioactive gas with a half life of 10.6 years. Kr-85 has many advantages over other tracers used in wind-tunnel studies. Its detection procedure is fairly simple and direct. It is diluted with air more than a thousand times before use to achieve a density nearly the same as that of air. The source strength can be controlled easily.

Its versatility makes possible the dosage measurements in the wind tunnel for which no other technique seems to be available at the present time.

2.2.6 Simulation of aircraft release - In order to simulate the elevated line source emitted by an aircraft, a traversing arrangement was designed as shown in Fig. 4. The schematic diagram of the tracer release system is presented in Fig. 5. The system can be described by considering the different components separately as follows.

a. Traverse. A quasi-instantaneous line source was produced by traversing a continuously emitting source of Kr-85 across the width of the

wind tunnel. In order to reduce the effect of the traversing arrangement on the flow patterns over the model, it was considered necessary to design a system which had the smallest possible dimensions normal to the flow and would, yet, be strong enough to carry the source smoothly. A streamlined brass plate 6 in. x 4 in. x 1/8 in. served as a carriage and could slide, by its four 1/2 in. long grooved supports, on two taut 16 gauge piano wires. These wires were tightened across the wind tunnel 12 in. above the wind tunnel floor and tension on them was adjusted to eliminate any oscillation due to the wind. The carriage was bound in a closed nylon thread loop which passed over four 1/4 in. O.D. sheaves. The spring tensioned loop along with the carriage was driven by a 15 in. diameter sheave belted to 1 HP D.C. variable-speed motor. A 1/8 in. I.D. brass tubing mounted on the carriage was used to release the tracer gas in the direction of flow. The height of release could be adjusted by raising or lowering the tube.

b. Kr-85 feed system. The tracer gas was fed to the moving source through a Mayon tubing supported along one of the piano wires with twenty-four 1/2 in. steel rings. As the carriage moved from one wall of the tunnel to the other, the extra length of Mayon tubing was retained outside the wind tunnel. This was done by displacing equal length of stainless steel wire cable over a 1 1/2 in. O.D. sheave set at a height of 15 ft above the carriage. An adjusted counter-weight at the end of the wire cable facilitated a smooth transfer of the tubing. A Fisher and Porter flowmeter was used to measure the rate of release which was kept constant throughout this study at 500 cc/min. Once the flow rate was adjusted, using a pressure regulator on the source cylinder and the flow meter, the feed was controlled by a 6V DC miniature electric valve placed in the line only 13 ft from the release point.

c. Sudden release and closure. For a quasi-instantaneous source experiment in the wind tunnel, it is very essential to turn the tracer gas on and off precisely when the traversing starts and stops. This was accomplished by providing 1/4 in. I.D. suction ports in front of the release point both at its starting and stopping positions. The suction was applied by a vacuum pump which discharged the gas withdrawn back to the wind tunnel at a section downwind from the city model. Thus release began as the source moved away from the suction port at the start and was stopped automatically as the source reached the other port. A rapid acceleration of the carriage to a predetermined speed was obtained by suddenly pressing an idler pully mounted on a lever against the slack motor belt. The carriage motion was most effectively stopped before the end suction port by applying brake to the 15 in. diameter sheave.

d. Disposal of Kr-85. The Kr-85 gas released into the wind tunnel was discharged from the building into the atmosphere through a vertical duct. Since its concentration was smaller than the maximum permissible concentration, no health hazard existed. Furthermore, there was no chance for the discharged gas to re-enter the tunnel and cause error due to fluctuations in background activity.

2.2.7 Sampling system - The concentration of a tracer released from a quasi-instantaneous source varies with time at a fixed point in space. A sampling device for such finite time releases usually is designed to obtain "dosage" --the time integral of the variable concentration. Thus the fundamental requirements for such a device are that it collects all tracer material passing by a sampling station and permits easy analysis of the total amount of tracer present in the sample. The system used in this study literally meets these requirements and is described under the same headings.

a. Collection equipment. Samples at an equivalent prototype height of 6 ft were drawn from the wind tunnel through 1/16 in. I.D. brass tubes and collected in glass bottles as shown in Fig. 6. The tube site was selected to permit isokinetic sampling. Twenty-five samples could be obtained at the same time for one release. The samples were collected by displacement over water. Each of the 25 collector bottles, initially filled with water, was connected to a common reservoir of water through a spherical connector to ensure equal pressure drop. A flowmeter between the connector and the reservoir monitored the volumetric rate at which water was withdrawn from the bottle. This flow rate controlled the sampling rate from the wind tunnel. In order to collect the samples, a predetermined negative air pressure was created above the water surface in the reservoir with a vacuum pump and the ball valve was opened. After the required volume (about 200 cc) of the sample was obtained, this valve was closed.

b. Analysis. Each sample was transferred into a cylindrical jacket around a Geiger-Mueller (G.M.) tube by a reverse process. Now the jacket was filled with water and pressure applied to air in the reservoir forced the sample from a collector bottle to transfer to the jacket. The volume of the jacket was exactly equal to that of the sample collected. Four jacketed G.M. tubes were used to facilitate transfer and analysis. Each G.M. tube was calibrated by using a gas of known concentration. The samples after transfer to G.M. tube jackets were counted by a scaler.

2.3 Fort Wayne City Model

A scale model of the city of Fort Wayne, Indiana was designed and built in the Fluid Dynamics and Diffusion Laboratory. The horizontal scale of the model was governed by the area to be modeled and the available

space in the environmental wind tunnel. In order to produce data comparable to the field study by Hilst and Bowne (1966), it was found necessary to model some of the surrounding rural area in addition to the city proper. Thus, a prototype width of 8 miles was required to be accommodated within 11 ft of the wind-tunnel width. A horizontal scale of 1:4000 satisfied this requirement and was used in the construction of the model. A vertical scale of 1:2000 was used to incorporate the vertical features like buildings. This exaggeration in the vertical was necessary because the building heights, if based on horizontal scales, were reduced so much that the model would behave as an "aerodynamically smooth" surface. The formalities of such a technique are discussed in the next chapter.

2.3.1 Roughness characteristics - The model base was made of 3/4 in. thick plywood. A detailed map of the city was enlarged to the scale of 1:4000 and was glued to the base. The model covered an area of 12 ft x 12 ft and was assembled from 9 pieces of 4 ft x 4 ft plywood. Figure 7 shows the area of the city covered by the model and diffusion sampling stations both in the field and in the model. Details of the high-rise buildings were derived from aerial photo maps and each building was modeled and fixed at the proper location in the downtown area. Buildings less than four stories high were modeled to appropriate height by simulating the entire city block as a single roughness element. An exact reproduction of the structure of a city block was considered unnecessary for three reasons. First, in and around downtown the structures are so close and knit with trees that a city block can be expected to behave as a single element. Second, this study being of an exploratory nature, an effort to model the fine details was uncalled for. Lastly, if a simplified geometrical modeling such as proposed could produce satisfactory results,

further development of wind-tunnel models as a tool for studying urban diffusion would be justified.

City blocks were cut out of masonite sheets to proper proportions and shape as dictated by the map and aerial photos. The rural area was modeled by placing coarse sandpaper (50 Grit) and isolated patches of higher roughness were made from coarser paper. Each of the features were selected to contribute to the true roughness behavior of the city.

2.3.2 Heat-island effect - This feature of the prototype was incorporated into the model by placing heat sources at the surface of the model. Nichrome wires were laid in four different circuits over the model as shown in Fig. 8. By changing the voltage across these circuits, the form of the surface temperature distribution in the model city could be controlled. Strips of fiberglass drapery cloth were placed beneath the nichrome wires along their entire length to prevent the model surface from being charred due to heat. The appreciable expansion experienced by the nichrome wires during heating was taken up by providing 0.1 in. O.D. tensioned wire springs at the two ends of each wire. Each time the voltage was applied to the heating wires, the model surface temperatures were allowed to reach a steady state before data collection.

2.4 Velocity-Profile Production Technique

A number of methods were tried to produce a velocity profile over the model similar to that in the field. The final arrangement was a grid of cardboard tubes 2 1/2 in. diameter which were placed longitudinally at the entrance section across the width of the tunnel in two layers. This technique has similar advantages as those presented by Lloyd (1966) for flat boards. Also, a 16 foot-length of the wind-tunnel floor between

these tubes and the model was covered with fine roughness (rice grains glued to plywood sheets).

III. SIMULATION OF URBAN ATMOSPHERE AND DESIGN OF MODEL

In order that the wind-tunnel model flow corresponds to those occurring in the field, it is essential that the two flows be dynamically similar. This similarity conditions are usually sought in the differential equations cribing motion in the prototype flow as well as in the model flow. The conditions of dynamic similarity of a frictionless atmosphere were first examined by Batchelor (1953). His important conclusion is that if the flow fields are such that pressure and density everywhere depart by small fractional smounts only from the values of an equivalent atmosphere in adiabatic equilibrium and if the vertical distances over which appreciable changes in velocity occur are small compared with those for which density variations are appreciable, the Richardson number is the sole parameter governing dynamical similarity. Nemoto (1961 a,b,c, 1962), Cermak et. al. (1966) and McVehil et. al. (1967) have considered a variety of simulation problems. It is generally agreed that in case of a thermally stratified flow of turbulent air in the surface layer, dynamical similarity would be achieved if the model satisifes the following conditions.

1. Geometrical similarity
2. Reynolds number equality
3. Richardson number equality
4. Approach flow similarity.

Effect of earth's rotation on flow in the atmospheric surface layer can be ignored as the convective accerlation dominates the Coriolis acceleration and the horizontal extent of the surface under consideration is rather small. Cermak et.al. (1966) point out that if the prototype lengths are less than 150 km, the Coriolis forces do not produce large

differences in flow patterns between model and prototype. The proposed Fort Wayne model covers only an area of 8 x 8 miles and thus qualifies for this simplification.

The above stated similarity criteria cannot, however, be satisfied simultaneously between the model and the prototype. This problem is not new in modeling practice and can be analyzed by considering the relative importance of the different conditions in dispute. In conclusion, we may have to resort to partial simulation when the consequences of non-duplication of certain similarity parameters is properly understood. The approach is that of making known and calculated approximations based on sound knowledge.

3.1 Reynolds Number and Geometrical Similarity

Reynolds-number similarity based on the viscosity of air is neither practical nor essential to the present modeling effort. Two alternatives have been offered by different authors. Nemoto (1961a) evolves an "eddy" Reynolds number defined as

$$R_e = \frac{UL}{K_m} \tag{1}$$

as a similarity parameter. It is obviously not a practical criterion because the eddy diffusivities are not known off hand in the field or in the wind tunnel. On the basis of assumptions of local isotrophy and identity of rates of energy dissipation in the two flows, Nemoto expresses the Reynolds number criterion for modeling wind velocity as

$$\frac{U_{\infty M}}{U_{\infty p}} = \left[\frac{L_M}{L_p}\right]^{1/3} \tag{2}$$

This is a much more plausible form of Reynolds number similarity and has the effect of scaling down the wind velocity instead of requiring it to be increased for the model as was the case with ordinary Reynolds number.

The above approach to Reynolds number similarity disregards the effects of surface terrain on flow phenomena. The fact that the turbulent flow of air in the surface layer over an urban area is invariably aerodynamical rough, opens up a new possibility. According to McVehil et.al. (1967) an aerodynamically rough flow is similar to any other aerodynamically rough flow irrespective of its velocity, roughness length and kinematic viscosity. In other words, the velocity of flow, roughness length and viscosity can be varied independently of each other. Thus if the flow over the model is rough, the Reynolds numbers need not be equal. On the other hand, it is essential that the surface features be sufficiently large and the Reynolds number sufficiently large for the model to guarantee that the flow will have the characteristics of a flow over an aero-dynamically rough surface.

The question whether a given surface produces an aerodynamically fully rough flow has been discussed by Sutton (1953) and Schlichting (1955). According to Sutton an aerodynamically rough surface is one in which the irregularities project into the flow enough to prevent the formation of a non-turbulent viscous layer, so that the motion is turbulent between the roughness elements. From Nikuradse's measurements on flow through pipes whose surfaces were uniformly covered with sand grains of height k_s, the criterion for fully rough flow was determined to be

$$\frac{u_* k_s}{\nu} > 75 \qquad (3)$$

where u_* is the friction velocity (defined as $\sqrt{\tau_o/\rho}$, τ_o being the surface shear stress and ρ the density of fluid) and ν is the kinematic viscosity. Nikuradse's surface roughness was so placed that a single length such as k_s was sufficient to describe its properties. For other surfaces like the model of the city of Fort Wayne, the number of such length parameters is increased. In addition to the height of the city blocks, some other lengths specifying their spacing must be considered. Schlichting (1936) simplified the problem by introducing a length called equivalent sand roughness k_s for such surfaces. He carried out experimental determination of k_s for a number of roughness types as a function of concentration of the roughness elements. Since then, several others have experimented with sharp edged roughness elements (see Koloseus and Davidian 1966). Such information makes it possible to use Nikuradse's test for roughness (as stated above) on the city model.

Geometrical similarity between the model and the prototype is realized if the spatial boundaries in the two bear the same ratio at the corresponding locations. As indicated in the description of the model, the wind-tunnel width fixes the horizontal scale of the model at 1:4000. Now if we adopt the same ratio to scale the vertical heights in the model, geometrical similarity will be satisfied; however, an average residential area city block with its buildings and trees (taken to be about 25 ft high) would scale down to 0.075 in. in the model. The concentration of the blocks, λ, is defined as the ratio of the sum of projected areas of the blocks normal to the wind direction, to the total floor area. Rouse (1965) and Koloseus and Davidian (1966) found, based on data from numerous sources, that a simple relation exists between the ratio of k_s

to actual height of roughness k_1 and the roughness concentration γ which is independent of the roughness shape and arrangement over the lower range of concentration, say, below 0.1. Estimate of concentration of blocks can be made from the map of the city. From three areas, selected at random, a rather uniform value of 0.022 for the concentration λ is obtained if the height of the blocks is scaled to 0.075 in. From Koloseus and Davidian (1966), equivalent sand roughness to height ratio against $\lambda = 0.022$ is

$$\frac{k_s}{mk_1} = 2.2 \tag{4}$$

where m is an indicator of relative surface rugosity taken to be equal to 0.88 for rectangular roughness. With $k_1 = 0.075$ in., Eq. (4) gives

$$k_s = 0.145 \text{ in.} \tag{5}$$

Using this estimate of k_s, the criterion for a rough surface (Eq. 3) may be checked after an approximate value for u_* has been established.

As is explained in the next section, Richardson-number similarity requires the wind velocity to be as low as practicable which is opposite to the need of keeping the flow over the model fully rough. The higher the velocity, the greater is the temperature differential required to produce the heat-island effect. The choice of wind velocity is thus limited to the minimum stable value attainable with the existing wind-tunnel propeller system. This velocity is 8 ft/sec and is used to evaluate the similarity criteria.

If the boundary layer over a flat plate is turbulent from the leading edge, the local skin-friction coefficient c_f' is given by Schlichting (1955) as

$$\frac{u_*^2}{U_\infty^2} = \frac{1}{2} c_f' = 0.0296 \quad (R_x)^{-1/5}$$

$$5 \times 10^5 < R_x < 10^7 \qquad (6)$$

where $R_x = \frac{U_\infty x}{\nu}$ and x is distance from the leading edge. If the model is placed 20 ft from the leading edge, $R_x = 10^6$ and from Eq. (6), $u_* = 0.345$ ft/sec. Using this value and k_s from Eq. (5), we get

$$\frac{u_* k_s}{\nu} = 26.1 < 75 \qquad (7)$$

According to Nikuradse's criterion given by Eq. (3), flow over a model scaled by 1:4000 vertically and horizontally is not aerodynamically rough.

There are only two alternatives available to improve upon the magnitude of $\frac{u_* k_s}{\nu}$ to ensure that the flow is fully rough. One is to augment u_* by increasing the wind velocity over the model and the other is to increase k_s. The former tends to make similarity of the heat-island effect impracticable and has to be discarded as a means of rectifying the situation. We are, thus, left with only one choice viz., to exaggerate the vertical scale of the model. The distorted models are not uncommon in hydraulics and ocean engineering laboratory studies. This compromise between geometrical and Reynolds number similarity is not expected to introduce any serious limitation if a fully rough flow is produced in the wind tunnel. Some encouragement for distorted models comes from the equations of motion of a turbulent atmosphere as brought out by Nemoto (1961). The degree of vertical exaggeration is related to K_x and K_z, the turbulent diffusivities in the longitudinal and vertical directions respectively, as

$$\alpha = \left[\frac{K_{xp}}{K_{xM}} \cdot \frac{K_{zM}}{K_{zp}}\right]^{1/2} \qquad (8)$$

where subscripts M and p stand for model and prototype. In the wind tunnel K_x and K_z are expected to be of the same order whereas in the field K_x is at least one order of magnitude bigger than K_z (see for example, Kao and Wendell 1968 and Orgill 1970). Thus a vertical exaggeration $\alpha = \sqrt{10} \simeq 3$ is permissible in modeling atmospheric flow.

Let us consider a vertical exaggeration of the model by a factor of 2 which, by definition, doubles the concentration of the city block. From Koloseus and Davidian (1966) $k_s = 0.58$ in. and surface Reynolds number is

$$\frac{u_* k_s}{\nu} = 104 > 75 \ . \qquad (9)$$

Thus Nikuradse's criterion is satisfied and the flow over the model is fully rough aerodynamically if a vertical scale 1:2000 is used.

3.2 Richardson Number Similarity

In order to model the heat-island effect, the bulk Richardson numbers must be equal for model and prototype. It is defined as

$$R_{i_B} = \frac{gL \ \Delta T_o}{U_o^2 \ T_a} \qquad (10)$$

where the subscript 'o' denotes the value of a quantity with respect to a reference height. Thus, U_o is the velocity at the reference height and ΔT_o is the temperature difference between the surface and the reference height, T_a denotes the average temperature, L the characteristic length of flow and g the gravitational acceleration. In this study, the entire thermal structure is considered to be developed by heat sources within the city; therefore, elevated inversions and lapses in the upstream flow are eliminated from consideration. The thermal

structure over the model and the prototype will be similar if

$$\left[\frac{gL\Delta T_o}{U_o^2\ T_a}\right]_M = \left[\frac{gL\Delta T_o}{U_o^2\ T_a}\right]_p \quad . \tag{11}$$

To start with, it is reasonable to assume that $(T_a)_M$, the average temperature in the model is the same as that for the prototype $(T_a)_p$, then the condition of similarity is

$$\Delta T_{oM} = \Delta T_{op} \left[\frac{L_p}{L_M}\right]\left[\frac{U_{oM}}{U_{op}}\right]^2 \quad . \tag{12}$$

In order to evaluate the temperature differential over the model ΔT_{oM}, we shall consider the specific field trial intended to be modeled. Of the six "reliable" trials analyzed by Csanady, Hilst and Bowne (1967), half are designated as stable and half as moderately stable. As the present study is limited to the consideration of a neutral approach flow, one of the near-neutral trial 65-06-G2 is selected for modeling. For simulating the vertical heat-island effect, a reference height equal to 100 ft is selected. From G.T. Tower temperature data, the temperature differential ΔT_{op} is found to be about 0.28°C. The ratio $(\frac{U_{oM}}{U_{op}})$ may be approximated by $(\frac{U_{\infty M}}{U_{\infty p}})$ since the velocity profile in the wind tunnel is also to be made similar to that in the field. For the trial under consideration, velocity at about 3000 ft in the field is on the average 26 ft/sec and can be taken to be comparable to the proposed wind-tunnel air speed of 8 ft/sec. Thus, the temperature differential in the wind tunnel is given by Eq. (12) as,

$$\begin{aligned} \Delta T_{oM} &= 0.28\ (2000)\ (\tfrac{8}{26})^2\ ^oC \\ &= 53.2^oC \simeq 96^oF \quad . \end{aligned} \tag{13}$$

Thus, the Richardson number over the model will be similar to that over Fort Wayne within the first 100 ft at the G.T. Tower if a temperature differential of about $100^{o}F$ is maintained in the model at the corresponding position.

If the surface of the model is to be heated by resistance filaments (nichrome wire), it is necessary to investigate the feasibility of this scheme. This can be done by evaluating the power needed to heat the model in order to maintain the design temperature differential over it. We shall, thus, have to consider the heat transfer from the model in all the three modes--convection, conduction and radiation.

1. Forced Convection--There will be a spatial distribution of temperature over the model and the total temperature differential between the surface air and the free stream may be in excess of $100^{o}F$. On the average, however, we may assume that the surface is maintained, say, at $150^{o}F$ above the ambient temperature (of, say, $60^{o}F$). The average heat-transfer coefficient, h_c, over a rough plate under forced convection is (see for example, Krieth 1967),

$$h_c = 0.037 \left[\frac{U_\infty L}{\nu}\right]^{0.8} \frac{k}{L} (Pr)^{0.33} \qquad (14)$$

where k and Pr are the thermal conductivity and Prandtl number for air, L is the length of heated surface which is about 6 ft in the model, and U_∞ is the freestream velocity 8 ft/sec. If the fluid properties are evaluated at

$$T_f = \frac{1}{2} (T_{surface} + T_\infty) = 135^{o}F \qquad (15)$$

Eq. (14) gives $h_c \simeq 1.8$ Btu/hr/ft$^2{}^{o}$F. Accordingly, the heat transfer from the model (area $\simeq$ 36 ft^2) due to forced convection is

$$q_1 = h_c(T_{surface} - T_\infty) \times \text{model area}$$

$$= 1.8\ (150) \times 36 \simeq 9{,}700\ \text{Btu/hr} \qquad (16)$$

2. Conduction--If there is a $1\frac{1}{2}$ in. thick layer of plywood between the heated surface and the bottom of the wind-tunnel floor which may be at near-ambient temperature, some of the heat will be conducted through the plywood and lost by convection through the room. Taking thermal conductivity k of plywood as 0.1 Btu/hr ft ^oF and floor temperature of, say, 100^oF, heat transfer due to conduction through the wind tunnel floor is

$$q_2 = \frac{A \quad k}{t_{plywood}} \quad (T_{surface} - T_{floor})$$

$$= \frac{36 \times 0.1}{1.5/12} \quad (110) \simeq 3{,}200\ \text{Btu/hr} \qquad (17)$$

3. Radiation--The model is nearly completely surrounded by the wind tunnel on one side such that the geometry factor, G, may be taken to be 0.5. The net rate of heat transfer is given by

$$q_3 = \sigma \varepsilon A G\ (T'^4_{model} - T'^4_{W.T.\ walls}) \qquad (18)$$

where σ is the Stefan-Boltzmann constant with a value of 0.171×10^{-8} Btu/sq ft $^oR^4$ and ε is the emissivity of a plywood surface and T' is the absolute temperature in degrees Rankine. Upon substitution of the relevant data, the heat transfer due to radiation is

$$q_3 = 0.171 \times 10^{-8} \times 0.83 \times 36 \times 0.5 (670^4 - 520^4)$$

$$\simeq 4{,}100\ \text{Btu/hr} \quad . \qquad (19)$$

4. Total Heat Transfer--The Total quantity of heat to be supplied to the model surface is

$$q = q_1 + q_2 + q_3 = 17{,}000 \text{ Btu/hr.} \tag{20}$$

The power required to produce a heat island effect over the model city comparable to that over the prototype is, therefore, about 5KW. In order to be able to control the surface temperature pattern, it is necessary to divide the model into smaller units. If four separate circuits are used, each will have to supply, on the average, 1.25KW. It is quite feasible to draw up to 2KW on 110 v supply outlets. As the power may have to be adjusted amongst the four circuits, the maximum power available per circuit was selected to be 1.75KW. Also, let n be the number of 6 ft long 20 gauge nichrome wires (resistance 6.5 ohms per ft) in parallel. If the maximum current is 20 amperes, then from

$$1{,}750 = (20)^2 \left(\frac{39}{n}\right) ,$$

is obtained

$$n = 9 \tag{21}$$

The density of the heating wires is to be in accordance with the recorded inventory of heat sources within the city.

3.3 Approach Flow Similarity

In addition to the various similarity parameters considered above, the boundary conditions in the field should be reproduced faithfully. Of special importance are upwind flow conditions and those at the upper boundary. If the velocity distributions are matched and turbulence levels are the same, it will not only satisfy the upwind requirements but also

take care of the boundary-layer thickness over the model. Moreover, the longitudinal pressure gradient in the ambient flow over the model should be adjusted zero as is the case in the field.

3.4 Diffusion Similarity

Once the similarity of flow is established, similarity in diffusion characteristics will follow if the linear dimensions of the source configuration are scaled properly. For example, the height of the quasi-instantaneous source in the wind tunnel should correspond to the best estimates of the airplance elevation. Csanady et.al. (1969) fix the cloud height at 75m for the trial 65-06-G2 which scales down to 1.48 in. in the model. Also the speed of the tracer release air craft is scaled to about 4 ft/min. One aspect of the field release method which cannot be readily simulated is the initial dispersion of the cloud in the wake of the air craft. This inability to model the initial conditions of the diffusion phenomena should not seriously affect similarity of distribution of the tracer material at distance downwind extending 10 - 20 times the source height.

IV. EXPERIMENTAL RESULTS AND DISCUSSION

In this chapter are presented the results of the measurements performed on the model of the city of Fort Wayne in the environmental wind tunnel at the Fluid Dynamics and Diffusion Laboratory of Colorado State University. The performance of the model in reproducing field flow characteristics is discussed. The model results are compared with those of the field trial 65-06-G2 (which was specifically modelled) and theory. Results of some visualization experiments, which were conducted before intensive model testing, are also presented.

4.1 Data

Model data were based on the values of test variables selected in the chapter on model design. Some of the data, which could not be presented wholly in graphical form, is arranged in tablular form in Appendix A. This is mostly the surface-dosage data obtained with and without incorporating the heat-island effect in the city model. All the vertical distributions are given only in graphical form. These include vertical temperature, velocity, turbulence and dosage data.

4.2 Approach Flow

The flow approaching the city area is characterized mainly by velocity and turbulence distribution in the vertical. For the velocity profile reproduction, tower data (G.T.) and balloon data (Site 2) formed a set which could be compared directly to wind-tunnel velocity data at the corresponding location. After many trials, the two profiles were matched as shown in Fig. 9. Although turbulence data are sparse in the field, a comparison of whatever data are available is essential from the point of view of assessing model behavior. Figure 10 shows the vertical

distribution of longitudinal turbulence intensity in the wind tunnel along with field data. The agreement between the field and wind tunnel velocity and turbulence intensity profiles approaching the city provides much encouragement for arriving at a satisfactory simulation of flow and diffusion near the city.

4.3 Flow Over the Model City

The model city modifies the approaching flow both in respect to velocity and temperature characteristics. Figure 11 shows the velocity distributions at WANE T.V., G.T. Tower and mid-city locations. Whereas the WANE and G.T. profiles are nearly alike, that over the mid-city differs considerably and the joint effect of roughness and heating extends to a height equivalent to 200 meters in the prototype. Longitudinal turbulence intensity at the city block top level registers an increase from 29% at WANE to 42% at G.T. near the downtown area as shown in Fig. 12. The effect of the roughness on turbulence intensity is more pronounced than that on mean velocity and has already reached about the 75 meter level at G.T. Figure 13 shows the development of vertical temperature profiles over the model. The location of vertical temperature profile stations is indicated on the surface temperature map. The shape of the heat island produced in the wind tunnel is depicted in Fig. 14 and is based on surface temperature data gathered at 50 locations. Although field data for the trial 65-06-G2 is available only at 10 locations, the rough picture of the heat island that emerges from them (Fig. 15) is remarkably similar to that obtained in the wind tunnel as shown in Fig. 14. This likeness in the heat-island shapes may be regarded as an evidence of the right interaction between the model geometry and the proper distribution of heat sources. Thus, flow over the city of Fort

Wayne is modelled well when the bulk Richardson numbers for model and prototype are equal at the city center.

4.4 Visual Observations

The dispersion of smoke plumes released at ground level upwind from the city was studied visually to observe if any spurious circulation patterns were present. The flow was found to be generally well behaved. In Fig. 16 are presented pictures of a smoke plume released at the start of the model upwind from WANE T.V. Tower. It is noticed that the plume experiences a sudden increase in its vertical spread as it passes over the city proper. Also, the lateral movement at the surface is seen to be along the streets. All this agrees generally with the field experience.

4.5 Diffusion Results and Comparison with the Field Data

The model diffusion results are first compared with the field data and then with the theory. All the dosage data is reduced to non-dimensional form for these comparisons by writing the non-dimensional dosage $\mathbb{D}$ as

$$\mathbb{D} = \frac{DU_h h}{Q} \tag{22}$$

where D is the observed dosage, U_h the wind velocity at the source height h and Q the source strength. Model quantities were controlled and were, thus, known precisely. There is, however, some uncertainty regarding h and Q values in the field. The adjusted figures for these parameters as given by Csanady et.al. (1967) are used in preference to those based on air-craft data.

The surface dosage measurements, made at 250 stations on the model, are presented in Fig. 17 in the form of iso-dosage lines. These iso-lines are based on five station dosage averages to smooth the variability of

the individual dosages and to highlight the general characteristics. The highest non-dimensional dosage occurs in the rural area and has a value of 0.36. Also the area covered by a dosage equivalent to the city maximum is much larger in the rural area then it is in the city.

A closed contour downwind from the downtown area can be attributed to mixing by the high-rise buildings which help to diffuse the higher concentration in the core of the plume to ground level. The lines up to 1 1/2 ft from the walls are obliterated as the end effects due to the finite length of the line source become important in this region. The iso-dosage lines are fairly parallel upwind from the city and far in the rural area (say, 5 miles from mid-city) beside it. Thus the effect of the city extends in the cross-wind direction up to about half the city width from the outskirts beyond which the two dimensionality of the flow and the line source diffusion remains intact.

A similar plot of iso-dosage lines from field data (based on five station averages) is shown in Fig. 18. No systematic conclusions can be drawn from these data as the dispersion over the city area does not distinguish itself as clearly from that over the rural area. A better picture of surface dosage distributions over these areas is obtained from Fig. 19 reproduced from Hilst and Bowne (1966). This represents an average of all the 70 field trials and is in qualitative agreement with the model pattern. A comparison of the non-dimensional surface dosages obtained in the model experiments and the field trial 65-06-G2 at the fourth sampling line is made in Fig. 20. The two lateral dosage distributions show remarkable similarity in exhibiting the effect of the city on the dispersion process. Both show a dip of nearly the same shape in the dosage variation downwind from the city. Ten station average

dosages, plotted in the same figure further illustrate the effect of the city. The field dosages, however, show much more variability than the model data.

The longitudinal variation of ground dosages in the model city and the prototype are presented in Fig. 21. Also imposed on the graph is a similar relationship for the model but without the heat-island effect. The ground-level dosage in the field rises much more rapidly with distance than that in the model and starts decreasing from the first sampling line downwind. This is rather a sudden fall of the tracer material to the ground and takes place upwind of the city. Csanady et.al. (1967) explained it to be due to turbulence generated by the rural area (indicating a roughness length z_o = 3M). Analysis by Hanna (1970) shows a value of 15 cm for z_o which seems more appropriate index of roughness over farmlands. It appears that the initial dispersion of the tracer in the wake behind the air-craft which could not be reproduced in the laboratory might have been responsible for transporting the material to the ground earlier than would be caused by rural area turbulence alone. The effect of the downdraft from the disseminating air craft in causing substantial increase in ground-level dosages has been recognized by Vaughan and McMullen (1963) and Vaughan (1965). In such circumstances, direct comparison with the field data is not possible near the source. Away from the release line, the model and prototype data indicate nearly the same rate of decrease of dosage with distance and is indicated more clearly in Fig. 22. This comparison is very significant in that the rate of decrease of dosage represents the total effect of the city (both roughness and heat island). Moreover, the two cases become equivalent, despite the downdraft anomaly, at large

distances from the source as the tracer tends to "forget" its initial position. Thus the model gives a better overall picture of the effect of the city on dispersion process by excluding the aircraft downdraft effect in the field tests. The comparison of the model curves for dosage variation with and without the inclusion of the heat island effects in the city, clearly shows the importance of the internal heating upon the dispersion over a city. The maximum dosage in the city due to an elevated source would be reduced if the heat island is not present but the rate of decrease of dosage would be much slower. In general, elevated releases over an urban complex cause greater ground-level dosages than similar releases over a flat terrain. This effect emphasizes the need for locating industrial plants with tall stacks away from the cities.

Some idea of the growth of plumes in the field and the model can be obtained by computing σ_z from Sutton's model. The non-dimensional ground dosage is related σ_z as

$$D_o = \sqrt{\frac{2}{\pi}} \frac{h}{\sigma_z} \exp\left[- \frac{h^2}{2\sigma_z^2} \right] \qquad (23)$$

For a given value of D_o, $\frac{h}{\sigma_z}$ and hence σ_z can be obtained from Eq. (23). Figure 23 shows a comparison of field and wind-tunnel rates of growth of the cloud vertically. The two sets of data match reasonably well away from the source.

4.6 Comparison with Theory

Presently there is no theory of diffusion of a passive substance which incorporates surface roughness inhomogeneity and the heat-island effect. However, it is of practical importance to investigate the

possibility of using theoretical results based on the assumption of horizontal homogeneity. This can be done by using the local value of variable flow characteristics like shear velocity, roughness length determined from the flow field at the position of interest. The comparison between wind-tunnel data and theoretical results will be limited to Smith's (1957) model. According to this model, the velocity and vertical diffusivity are assumed to be distributed as follows:

$$\frac{U}{U_h} = \left[\frac{z}{h}\right]^{\alpha} \tag{24}$$

and

$$\frac{K_z}{K_h} = \left[\frac{z}{h}\right]^{1-\alpha} \tag{25}$$

(K_h is the vertical diffusivity at source height, h). The solution of the two-dimensional diffusion equation for non-dimensional dosage $\mathbb{D}$ is then given by

$$\mathbb{D} = \frac{DU_h h}{Q} = \frac{\zeta^{\alpha/2}}{(1+2\alpha)\xi} \exp\left\{-\frac{1+\zeta^{(1+2\alpha)}}{(1+\alpha)^2\xi}\right\} I_{-\frac{\alpha}{(1+2\alpha)}}\left\{\frac{2\zeta^{(1+2\alpha)/2}}{(1+2\alpha)^2\xi}\right\} \tag{26}$$

where Q = source strength (μci/cm),

D = mean dosage (μci-min/cc),

$\zeta = \frac{z}{h}$ = non-dimensional height, and

$\xi = \frac{K_h x}{U_h h^2}$ = non-dimensional longitudinal distance,

I = Modified Bessel function of the first order.

Variation of ground-level dosage is found from Eq. (26) to be

$$D_o = \frac{(1+\alpha)^{-1/(1+2\alpha)}}{\Gamma(\frac{1+\alpha}{1+2\alpha})\xi^{(1+\alpha)/(1+2\alpha)}} \exp\left[-\frac{1}{(1+2\alpha)^2\xi}\right] . \qquad (27)$$

Thus both vertical and ground level dosage distribution can be obtained if an estimate of α and K_h is available. From the velocity profiles over the model an average value of 0.2 for α is obtained. The reference diffusivity may be expressed as

$$K_h = \frac{u_*^2 h}{\alpha U_h} \qquad (28)$$

on the assumption of a constant shear stress. The estimate of shear stress is also obtained from the velocity profiles.

The comparison of ground-level dosages observed over the model with those predicted from Smith's equation in Fig. 24 shows good agreement between model derived and theoretical values. Dosages at the second sampling line are not in good agreement--probably because this is a region behind a step change in roughness. The vertical profiles of dosage at the beginning and the end of the city (sampling lines 1 and 5) are compared with theoretical values in Figs. 25 and 26. The agreement is remarkable at the first sampling line in that the maximum dosages match rather well. The position of the center of the cloud observed in the wind tunnel is slightly lower than that predicted. At the end of the city a substantial difference in character of the two distributions exists. Here the thermal effect appears to modify the vertical diffusion rates and they are not accounted for in the Smith formulation.

V. CONCLUSIONS

The possibility of modeling urban atmospheres and diffusion was explored by reproducing characteristics of flow over the city of Fort Wayne, Indiana in a wind tunnel. The dynamic similarity between wind tunnel and natural full-scale flows was achieved by designing the model such that flow over it was fully rough in an aerodynamic sense and the Richardson numbers were the same. The condition of fully rough flow was considered more crucial than strict geometrical similarity which was compromised for by exaggerating the vertical scale. In addition, the approach flow in the model was made to be similar to the atmospheric boundary layer.

The heat-island pattern in the wind tunnel was found to be similar to that in the field, which is good evidence that the model geometry and heat-source distribution interacted in a similar manner in the two cases. The surface-dosage measurements lead to the same general conclusions as the field data. The highest dosages occur in the rural area. The high-rise buildings tend to cause a local region of high dosages. The effect of the city extends in the cross-wind direction up to about half the city width from the outskirts beyond which the two dimensionality of flow remains intact. The rate of decrease of dosage at street level, far from the source, follows the same trend for model and full-scale data. The vertical and ground-level dosage distribution compares well with Smith's (1957) analysis.

A method of dosage determination is evolved for analyzing quasi-instantaneous source diffusion. Also the method of heating the model surface with nichrome-wire heating elements offers great versatility in producing thermal stratifications in the wind tunnel.

The present study did not include effects from undulation of the terrain and the approach flow was considered neutral. Furthermore, no attempt was made to model the climatic variation other than wind and temperature. The agreement found in flow and diffusion data for the model and the full-scale natural flow indicate that these complicating features can be studied by means of physical modeling.

The results of this study have proved that it is possible, at least for neutral approach flows, to simulate the flow over complex surface such as a city and obtain useful information, relatively inexpensively, on urban diffusion. This investigation opens the way for studies of air-pollution problems for purposes of urban planning. The location of industrial sites and power-generation complexes relative to major topographical features, the location of freeways through existing cities, the grouping of tall buildings in an urban-development program, or the location of an entirely new city relative to topographic features to minimize air pollution potentials under adverse meteorological conditions can be studied systematically.

REFERENCES

Batchelor, G. K. (1953), "The Conditions for Dynamical Similarity of Motions of Frictionless Perfect-Gas Atmosphere." Quarterly Journal of Royal Meteorological Society, Vol. 79, pp. 224-235.

Cermak, J. E., Sandborn, V. A., Plate, E. J., Binder, G. H. Chuang, H., Meroney, R. N., and Ito, S. (1966), "Simulation of Atmospheric Motion by Wind Tunnel Flows," Fluid Dynamics and Diffusion Laboratory Report CER66-17, Colorado State University.

Corrsin, S. (1949), "Extended Applications of the Hot-Wire Anemometer," NACA Tech. Note 1864.

Csanady, G. T., Hilst, G. R., and N. E. Bowne (1967), "Turbulent Diffusion From a Cross-Wind Line Source in Shear Flow at Fort Wayne, Indiana," Atmospheric Environment, Permagon Press, Vol. 1, pp. 79-99.

Davis, M. L. (1968), "Modeling Urban Atmospheric Temperature Profiles," Ph.D. Dissertation, Department of Civil Engineering, University of Illinois, Urbana, Illinois.

Hanna, S. R. (1970), "Turbulence and Diffusion in The Atmospheric Boundary Layer Over Urban Areas," Seminar presented at Syracuse U., Feb. 1970.

Hilst, G. R., and Bowne, N. E. (1966), "A Study of the Diffusion of Aerosols Released from Aerial Line Sources Upwind of an Urban Complex." Final Report, Contract No. DA42-007-AMC-38(R), to Dugway Proving Ground. The Travelers Research Center, Inc., Hartford, Conn.

Kao, S. K., and Wendell, L. K. (1968), "Some Characteristics of Relative Particle Dispersion in the Atmosphere's Boundary Layer," Atmospheric Environment, Pergamon Press, Vol. 2, pp. 397-407.

Koloseus, H. J., and Davidian, J. (1966), "Roughness-Concentration Effects on Flow Over Hydrodynamically Rough Surfaces," U.S. Geological Survey Water-Supply Paper 1592-C, D.

Kovasnay, L. S. G. (1953), "Turbulence in Supersonic Flow," Journal of Aeronautical Sciences, Vol. 20, pp. 657-674.

Kreith, F. (1962), "Principles of Heat Transfer," International Text Book Co., Scranton, Penn.

Lloyd, A. (1966), "The Generation of Shear Flow in a Wind Tunnel," Quarterly Journal of Royal Meteorology, Vol. 93, pp. 79-96.

McVehil, G. E., Ludwig, G. R., and Sundaram, T. R. (1969), "On the Feasibility of Modeling Small Scale Atmospheric Motions," Cornell Aeronautical Laboratory, Inc., CAL Report No. ZB-2328 P-1.

Myrup, L. O. (1969), "A Numerical Model of the Urban Heat Island," Journal of Applied Meteorology, Vol. 8, pp. 908-918.

Nemoto, S. (1961a), "Similarity Between Natural Wind in the Atmosphere and Model Wind in a Wind Tunnel (I)," Papers in Meteorology and Geophysics, Vol. 12, No. 1, pp. 30-52.

Nemoto, S. (1961b), "Similarity Between Natural Wind in the Atmosphere and Model Wind in a Wind Tunnel (II)," Papers in Meteorology and Geophysics Vol. 12, No. 2, pp. 117-128.

Nemoto, S. (1961c), "Similarity Between Natural Wind in the Atmosphere and Model Wind in a Wind Tunnel (III)," Papers in Meteorology and Geophysics, Vol. 12, No. 2, pp. 129-154.

Nemoto, S. (1962), "Similarity Between Natural Wind in the Atmosphere and Model Wind in a Wind Tunnel (IV)," Papers in Meteorology and Geophysics, Vol. 13, No. 2, pp. 171-195.

Orgill, M. M. (1970), Personal Communication on Magnitude of Diffusivities.

Rouse, H. (1965), "Critical Analysis of Open Channel Resistance," Proceedings of the American Society of Civil Engineers, Journal of the Hydraulics Division, Paper 4387.

Schlichting, H. (1936), "Experimentelle Untersuchungen zun Rauhigkeit's Problem," Ingenieur-Archiv., Vol. 7, No. 1, pp. 1-34 [Translation, NACA Tech. Memo, 823, April 1937].

Schlichting, H. (1960), "Boundary Layer Theory," Fourth Edition, McGraw-Hill, New York.

Smith, F. B. (1959), "The Diffusion of Smoke from a Continuous Elevated Point Source into a Turbulent Atmosphere," Journal of Fluid Mechanics, Vol. 2, pp. 49-76.

Sutton, O. G. (1953), "Micrometeorology," McGraw-Hill, New York.

Turner, D. B. (1964), "A Diffusion Model for an Urban Area," Journal of Applied Meteorology, Vol. 3.

Vaughan, L. M. (1965), "Further Analysis of Intermediate-Scale Aerosol Cloud Travel and Diffusion Data from a Low-Level Aerial Line Releases," Technical Report No. 117, Aerosol Laboratory, Metronics Associates, Inc., Pala Alto, California.

Vaughan, L. M., and McMullen, R. W. (1963), "Intermediate Scale Aerosol Cloud Travel and Diffusion from Low-Level Aerial Line Releases," Technical Report No. 97, Aerosol Laboratory, Metronics Associates, Inc., Pala Alto, California.

APPENDIX A

NON-DIMENSIONALIZATION OF DOSAGES

Laboratory Data

Concentration of release gas = 164 μci/cc

Length of release = 10.64 ft.

Average traversing time = 3 min.

Rate of flow = 500 cc/min.

Rate of release = 164 μci/cc x 500 cc/min.

= 82 mci/min.

Total quantity released = 82 mci/min. x 3 min.

= 246 mci

Source Strength, Q = $\frac{246 \text{ mci}}{10.64 \text{ x } 30.48 \text{ cm}}$ = 760 μci/cm

Height of release, h = 1.5 in. = 3.81 cm

Wind velocity at release ht., U_h = 4 ft/sec = 7,320 cm/min.

Non-dimensionalizing dosage = $\frac{Q}{U_h h}$

$= \frac{760 \text{ x } 10^6 \text{ μμci/cc}}{7{,}320 \text{ cm/min x } 3.8 \text{ cm}}$

$= 2.72 \text{ x } 10^4$ μμci-min./cc

Field Data

For Run 65-06-G2 (from Csanady et.al. 1967)

h = 75 m

$\frac{Q}{U_h}$ = 17,400 particles-min/m/liter

Non-dimensionalizing dosage = $\frac{Q}{U_h h}$ = 232 particle-min/liter

APPENDIX B
END EFFECTS DUE TO FINITE LENGTH SOURCE

The width over which the tracer was released was less than the model width and thus some sampling points over the model did not "see" the whole width of the transient plume. The integration of the plume concentration for such locations was partial and identification of such regions was essential. A continuous source experiment was performed to determine the lateral spread of a plume release at the height used for quasi-instantaneous source experiments. Fig. 27 shows the variation of ground concentration from such a release upwind of the city. The width of the plume at the ground is approximately 2 feet at the 5th sampling line. The traversing source started and stopped at about 8 inches from the wind tunnel walls. The region of partial integration is identified as that within 1'-8" from the walls as shown in Fig. 17. Thus, the data over the center 9 feet of the model can be regarded as that due to an infinite line source.

TABLE I

Surface Dosages with Heat Island (μμci-min/cc)

Sampling* Station	Sampling Line 1 +(x=1.03 ft)	Sampling Line 2 (x=2.87 ft)	Sampling Line 3 (x=4.33 ft)	Sampling Line 4 (x=6.16 ft)	Sampling Line 5 (x=8.00 ft)
1	-	-	-	-	-
2	535	2915	4880	4125	5769
3	2325	6785	9320	7150	7362
4	555	7360	9575	6940	7032
5	530	6775	7500	8950	6538
6	520	8945	8440	9950	5494
7	790	7170	9075	9090	4560
8	1300	7485	9765	9050	5329
9	1170	6240	11445	7725	5989
10	1140	7345	9700	9730	6593
11	445	7025	10765	8065	6153
12	1230	5365	11410	7530	6648
13	470	9320	10270	6650	6485
14	1320	8470	9930	9410	5714
15	620	7545	8495	7975	6923
16	335	8795	8770	9040	6043
17	650	6980	7495	10210	5054
18	800	7095	8360	9170	5879
19	1420	6930	6655	8675	6925
20	1115	6640	10500	7715	6868
21	1185	6185	7990	8275	6868
22	565	6875	7465	8280	5934
23	765	595	9095	6500	5000
24	1335	9515	7585	6970	-
25	1615	10840	8630	8670	4395
26	1460	8680	9120	8540	1373
27	711	7220	9555	8400	5770
28	787	9150	11065	7970	5840
29	200	9110	9380	6585	4875
30	1395	9450	5430	6050	5040
31	749	8115	9370	6230	7580
32	2320	8925	7975	6610	7615
33	1509	6360	6155	6640	7015
34	467	7550	7725	7400	6525
35	1319	8115	7055	6325	5780
36	1026	6200	7645	9150	5040
37	924	7270	7095	8815	5610
38	1390	8600	7320	7720	5525
39	1047	9095	7865	5295	4275
40	656	9485	7615	4910	4210
41	412	5145	7095	4720	5165
42	2112	1440	4475	5740	5825
43	-	-	-	6400	5855
44	-	-	-	5940	5750
45	-	-	-	5244	-
46	-	-	-	4532	-

*Sampling stations are numbered starting from the north east edge of the city (see Fig. 7).

+ x is the longitudinal distance measured in feet from the source.

TABLE II

Surface Dosages Without Heat Island (μμci-min/cc)

Sampling* Station	Sampling Line 1 +(x=1.03 ft)	Sampling Line 2 (x=2.87 ft)	Sampling Line 3 (x=4.33 ft)	Sampling Line 4 (x=6.16 ft)	Sampling Line Line 5 (x=8.00 ft)
1	-	-	-	2400	-
2	-	1595	1707	5766	3095
3	0.0	5959	5397	7176	3545
4	2462	5793	7319	7118	3980
5	0.0	4447	5951	7278	5386
6	271	6011	5960	6377	5151
7	374	6127	8690	6572	5408
8	1303	6651	7403	7688	4715
9	369	8351	8230	8707	5245
10	1802	6942	7143	7167	6132
11	445	7623	6138	6260	5565
12	241	8145	6214	6359	6038
13	1415	7056	6078	5910	6244
14	723	6091	7825	5193	5255
15	255	5039	6266	7430	6081
16	605	5880	8432	7121	6081
17	860	8204	7726	7588	6277
18	1305	6413	7292	8696	5625
19	659	6837	6836	6996	5574
20	317	8866	7154	8019	5810
21	977	8554	7145	8848	5571
22	1074	5590	6760	7319	6526
23	445	5935	8335	6158	6091
24	295	8210	8576	6708	5679
25	408	7509	6211	8905	5484
26	1379	7050	6165	6176	4960
27	1012	5239	7197	7261	6016
28	105	5674	6005	6926	6045
29	758	6111	5905	5989	5098
30	946	6349	5565	6662	5415
31	1609	7995	8712	5858	4845
32	2546	7821	7127	5093	4615
33	1297	7957	8085	4702	5415
34	385	8921	7667	5696	5418
35	1148	8765	7414	6486	5098
36	1680	7335	8286	6377	5538
37	648	5957	8730	6668	5750
38	1268	7881	8370	6363	5131
39	1835	7037	8734	5003	5386
40	1411	6168	4102	6247	8188
41	458	5796	1791	6241	5669
42	0	2823	347	6936	5571
43	-	-	-	8221	5594
44	-	-	-	3868	1297
45	-	-	--	1625	-
46	-	-	-	250	-

*Sampling stations are numbered starting from the northeast edge of the city (See Fig. 7)

+ x is the longitudinal distance measured in feet from the source.

TABLE III

ELEVATED FIXED SOURCE CONCENTRATIONS AT GROUND LEVEL

WITH HEAT ISLAND

Q = 1550 μci/min

Sampling Line	*Y (in)	Concentration (μμci/cc)	Sampling Line	Y (in)	Concentration (μμci/cc)	Sampling Line	Y (in)	Concentration (μμci/cc)
1	+4.5	2	7A	+7.0	0	2	+8.0	0
+(x=1.03 ft)	+2.5	19	(x=1.95 ft)	+5.0	32	(x=2.87 ft)	+7.0	0
	+1.5	96		+3.0	161		+5.0	90
	+0.5	230		+2.0	478		+3.0	450
	-0.5	247		+1.0	905		+2.0	767
	-1.0	193		0	922		+1.0	907
	-1.5	102		-1.0	1011		0	890
	-2.0	71		-2.0	685		-1.0	910
	-2.5	38		-2.5	365		-2.0	799
	-4.0	0		-4.25	106		-4.0	535
				-5.25	23		-6.0	35
				-7.25	7		-8.0	22
				-9.25	0			
3	+12.0	0	4	+12.0	0	5	+12.0	18
(x=4.33 ft)	+9.0	15	(x=6.16 ft)	+9.0	0	(x=8.00 ft)	+9.0	84
	+6.0	69		+5.0	85		+6.0	180
	+4.0	234		+3.0	240		+4.5	247
	+3.0	431		+1.0	400		+3.0	289
	+2.0	520		0	457		+1.5	301
	+1.0	576		-1.0	461		0	279
	0	758		-2.0	451		-1.0	321
	-1.0	843		-3.0	321		-3.0	225
	-3.0	663		-4.0	148		-6.0	130
	-5.0	331		-6.0	29		-9.0	41
	-6.5	62		-9.0	12		-12.0	6
	-9.5	10		-12.0	0			

*Y is the model distance measured in inches from the centreline of the plume. Positive towards north

+ x is the longitudinal distance measured in feet from the source.

TABLE IV

SURFACE AIR TEMPERATURES OVER THE MODEL

Sampling Line	*Y' (in)	Temp. (°F)	Sampling Line	Y' (in)	Temp. (°F)	Sampling Line	Y' (in)	Temp. (°F)
1	28	77.5	2	16	60.0	3	13	57.5
+(x=1.03 ft)	40	100.5	(x=2.87 ft)	28	61.0	(x=4.33 ft)	25	58.0
	52	77.5		40	62.0		37	65.5
	64	95.0		52	83.5		51	156.5
	76	91.5		77	210.5		67	149.0
	88	135.5		98	201.5		79	118.0
	100	164.5		111	148.0		92	132.3
	112	103.0		131	176.0		107	158.5
	124	66.5		143	58.0		119	123.5
	139	60.5					127	120.0
4	19	57.5	5	16	56.0			
(x=6.16 ft)	31	58.2	(x=8.00 ft)	40	57.0			
	43	61.0		55	66.5			
	55	73.0		67	62.5			
	67	72.6		79	78.0			
	79	172.0		91	88.5			
	91	215.0		103	68.2			
	100	104.5		116	66.4			
	112	70.3		124	63.2			
	127	70.0						

+x is the longitudinal distance measured in feet from the line source.

*Y' is the distance measured in inches from the northeast edge of the model.

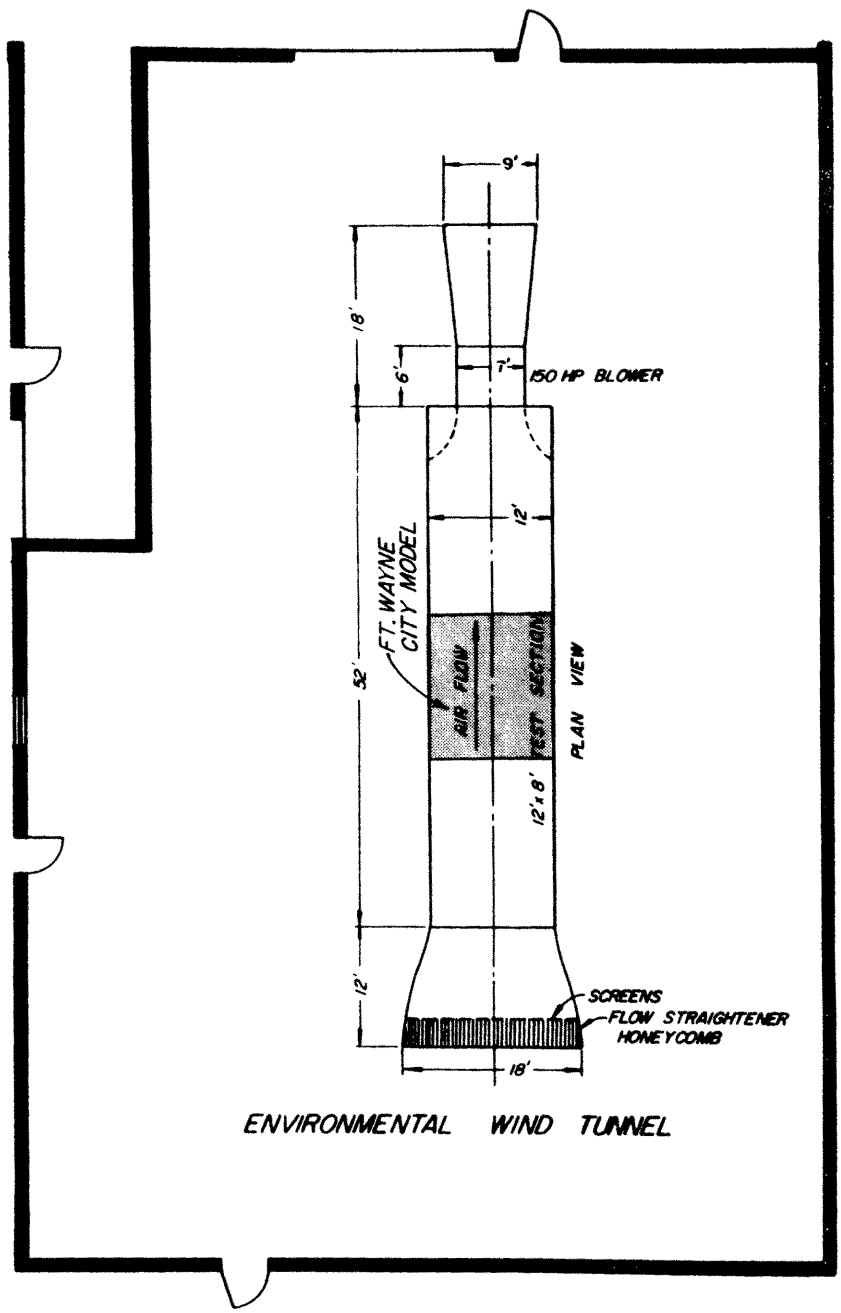

Figure 1. Environmental Wind Tunnel

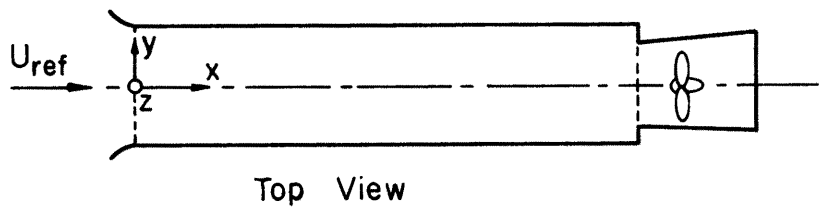

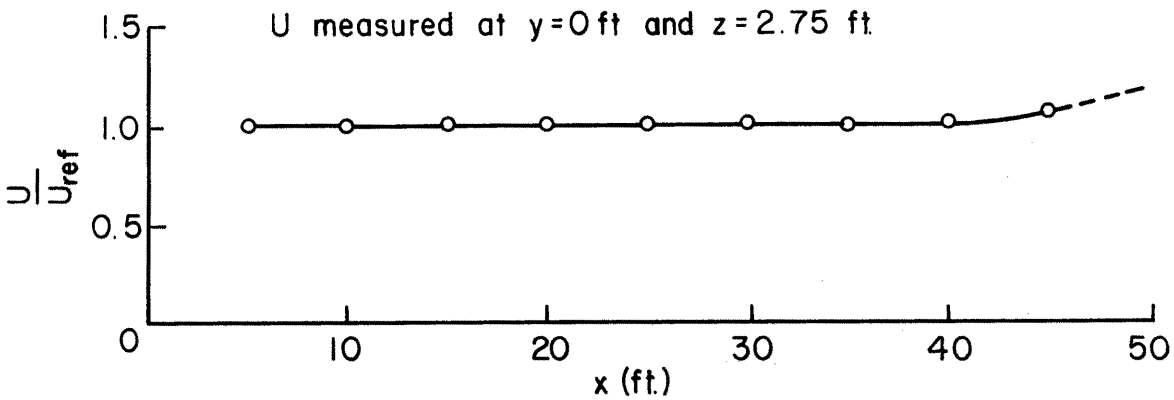

Figure 2. Free Stream Velocity Variation in the Longitudinal Direction

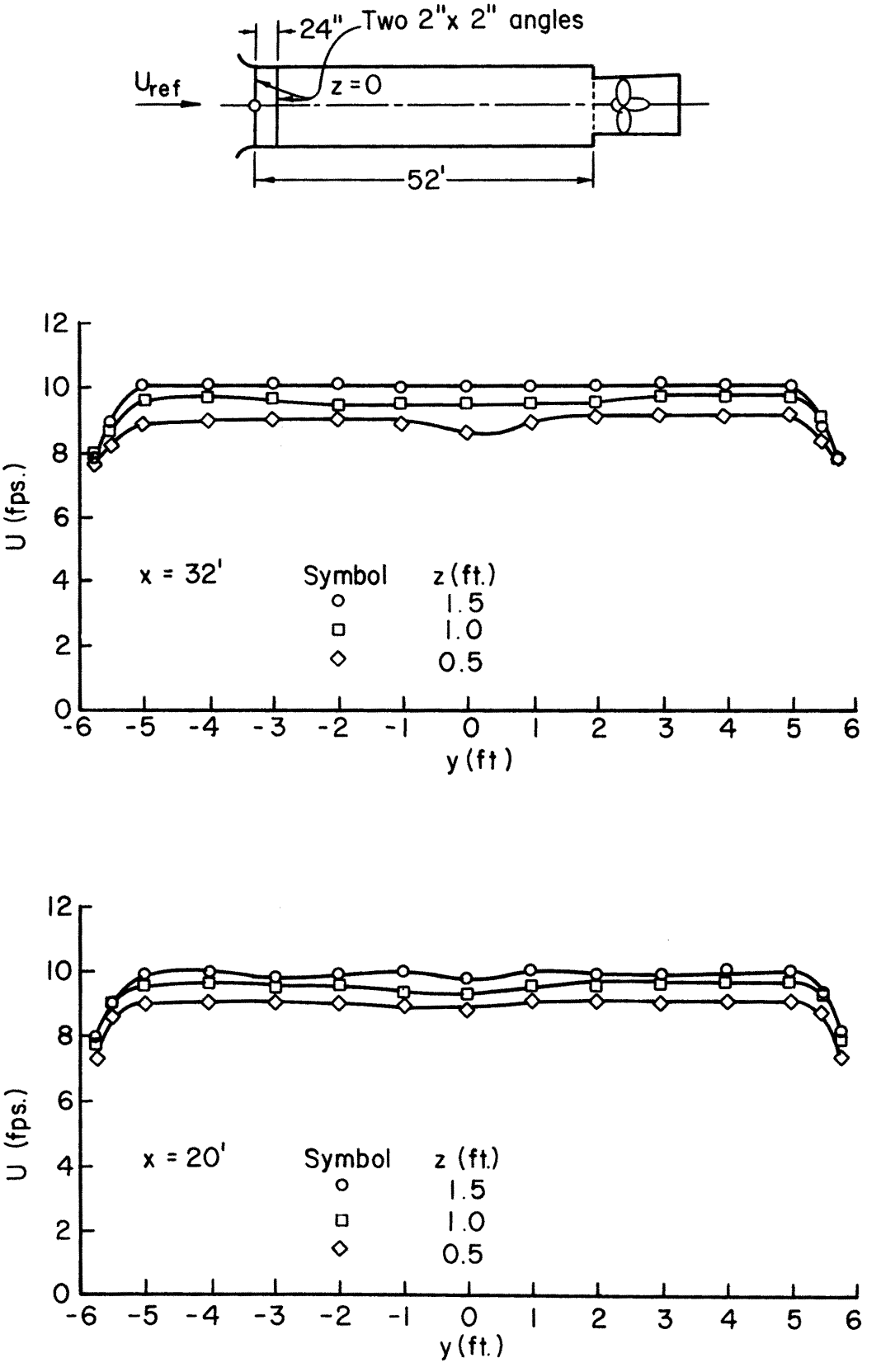

Figure 3. Transverse Velocity Distribution at x=20 and 32 ft

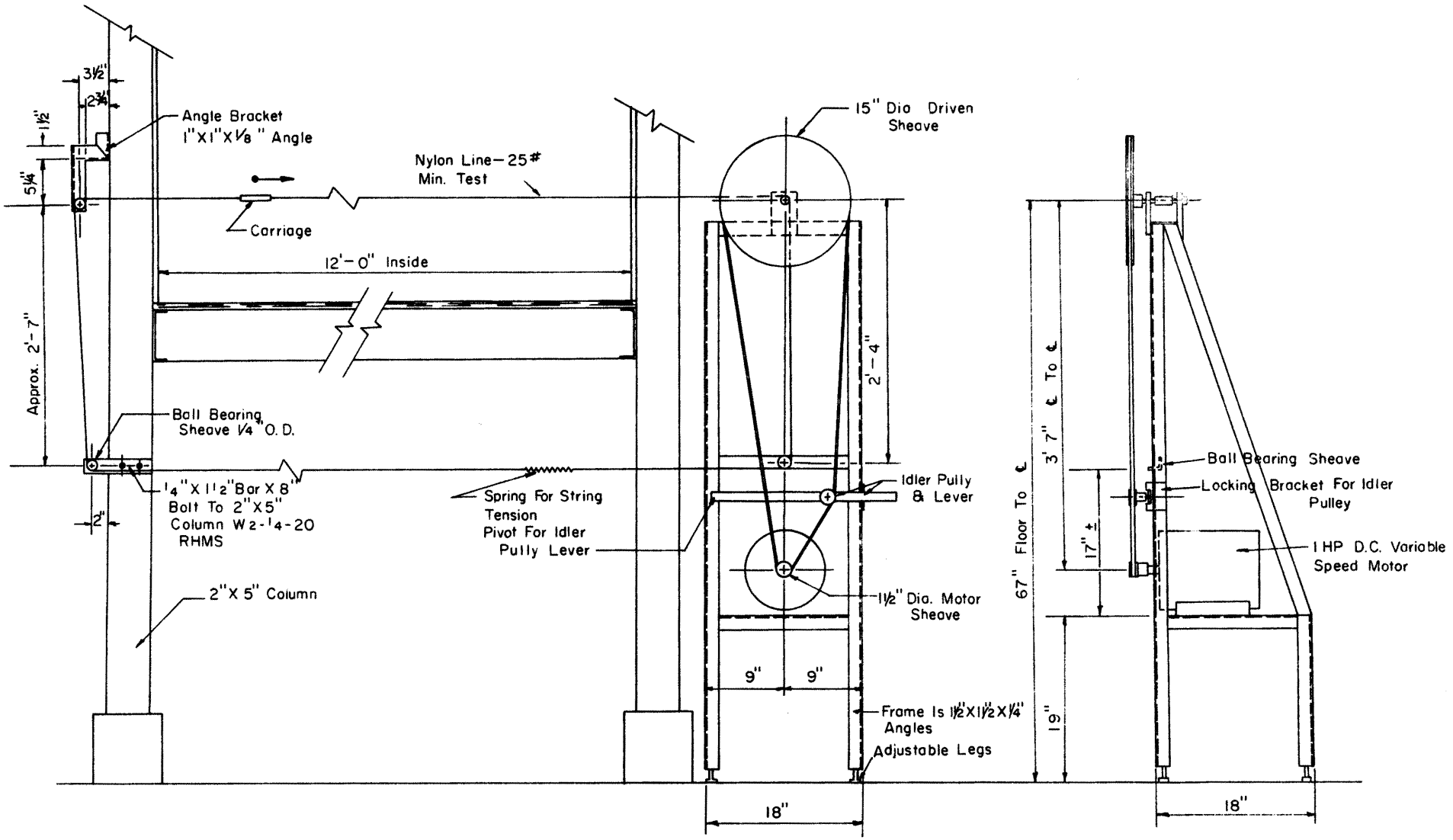

Figure 4. Traversing Arrangement

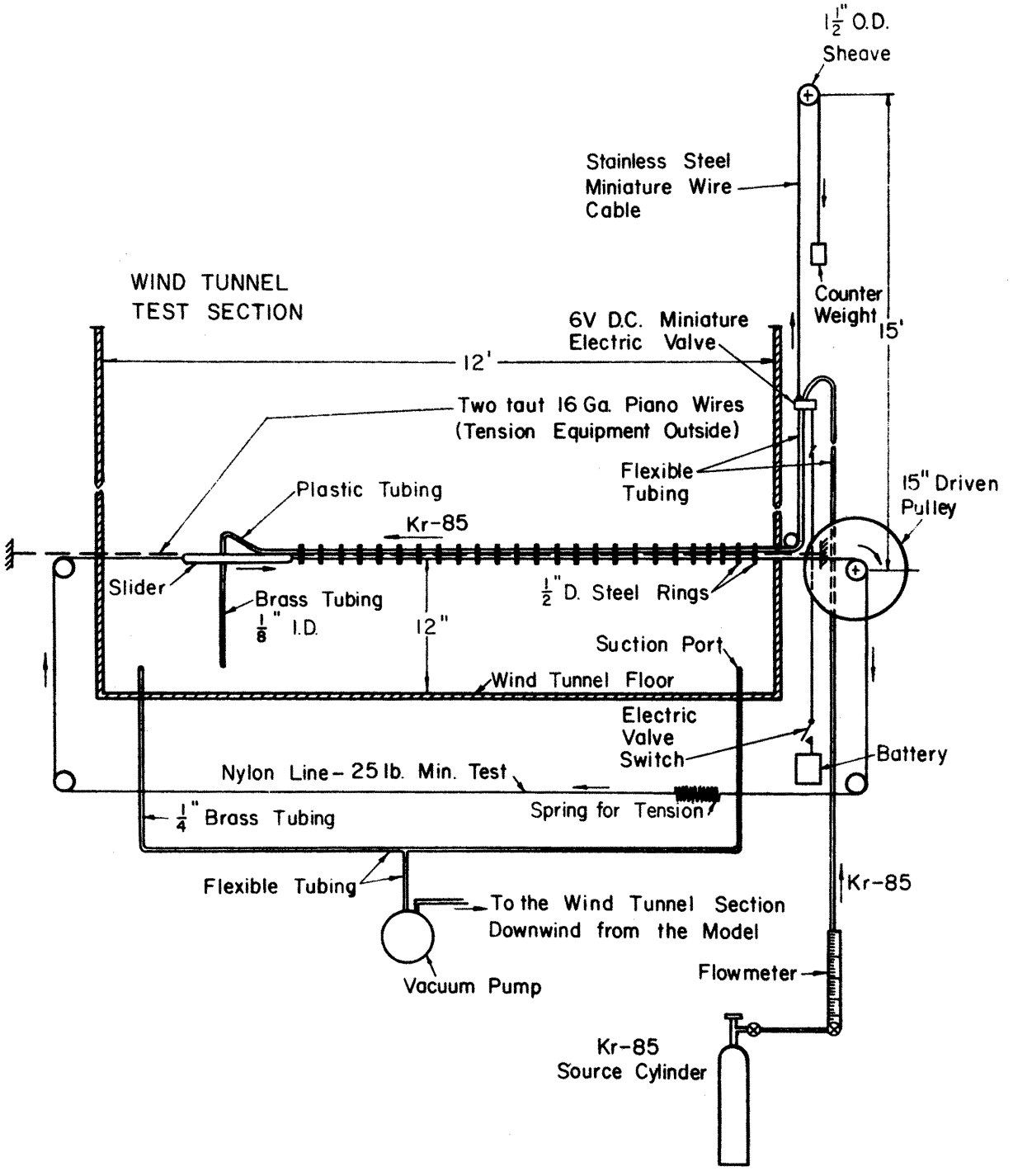

Figure 5. Schematic Diagram of the Tracer Release System

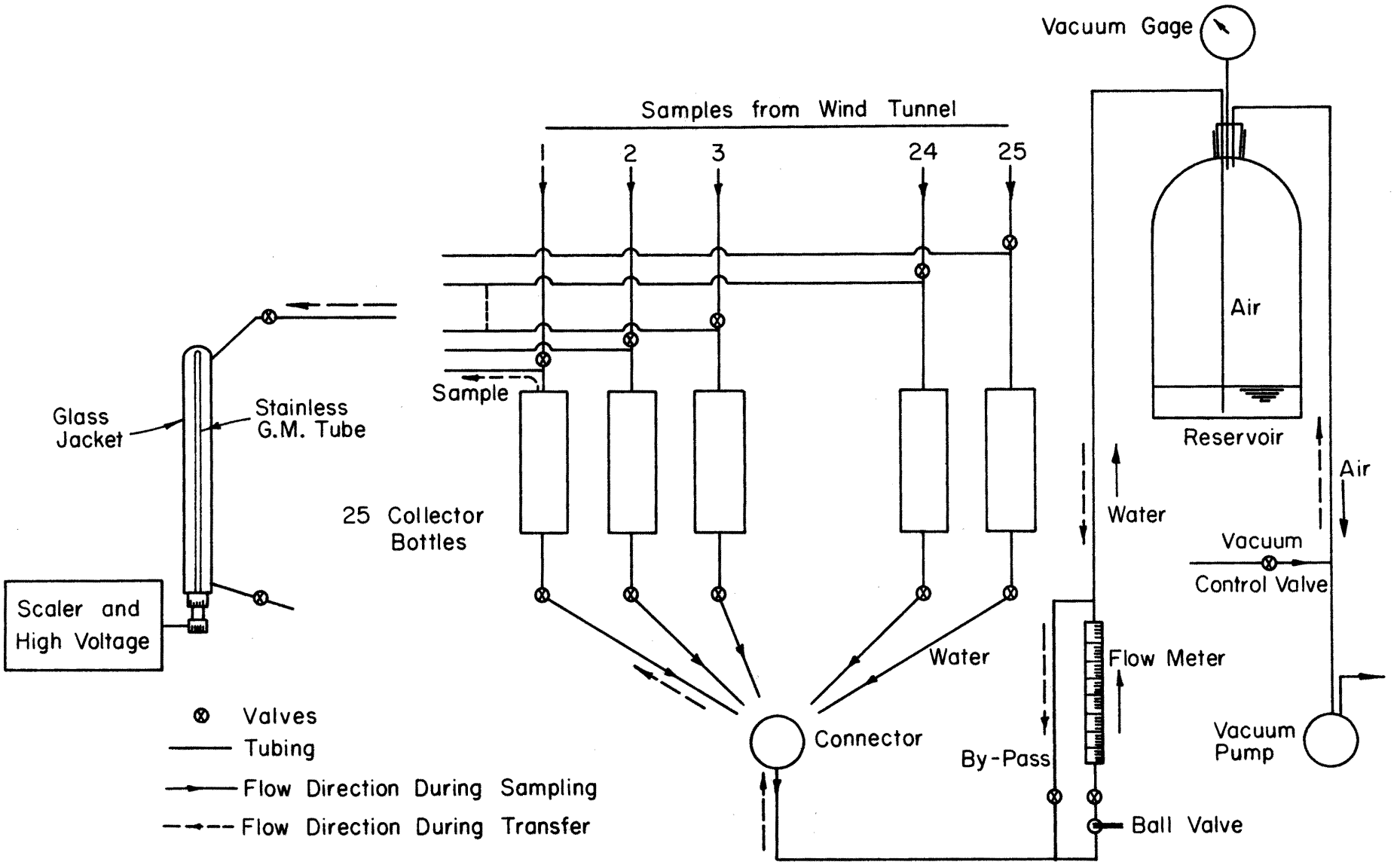

Figure 6. Sampling System

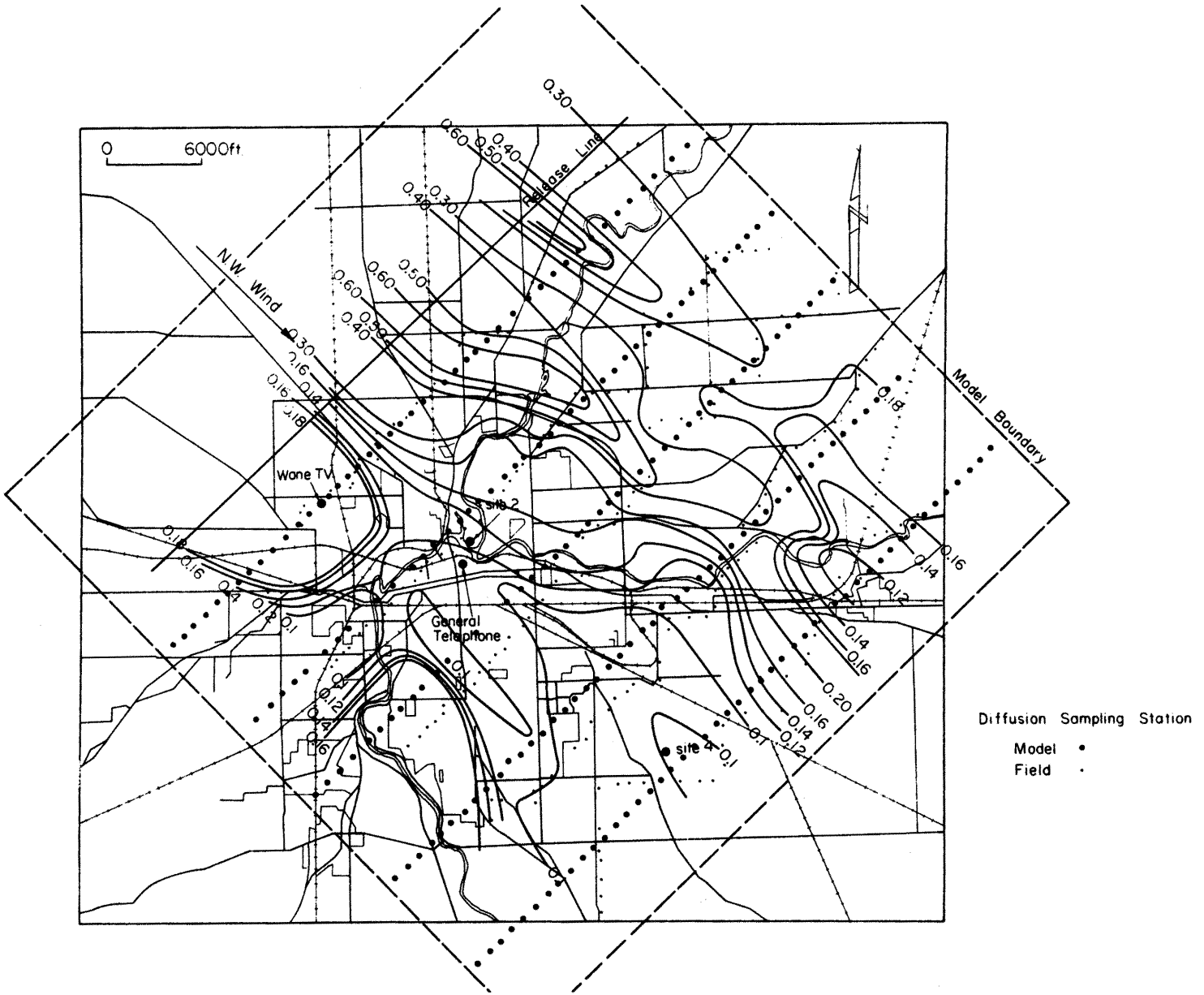

Figure 7. Model Lay-Out and Diffusion Sampling Stations

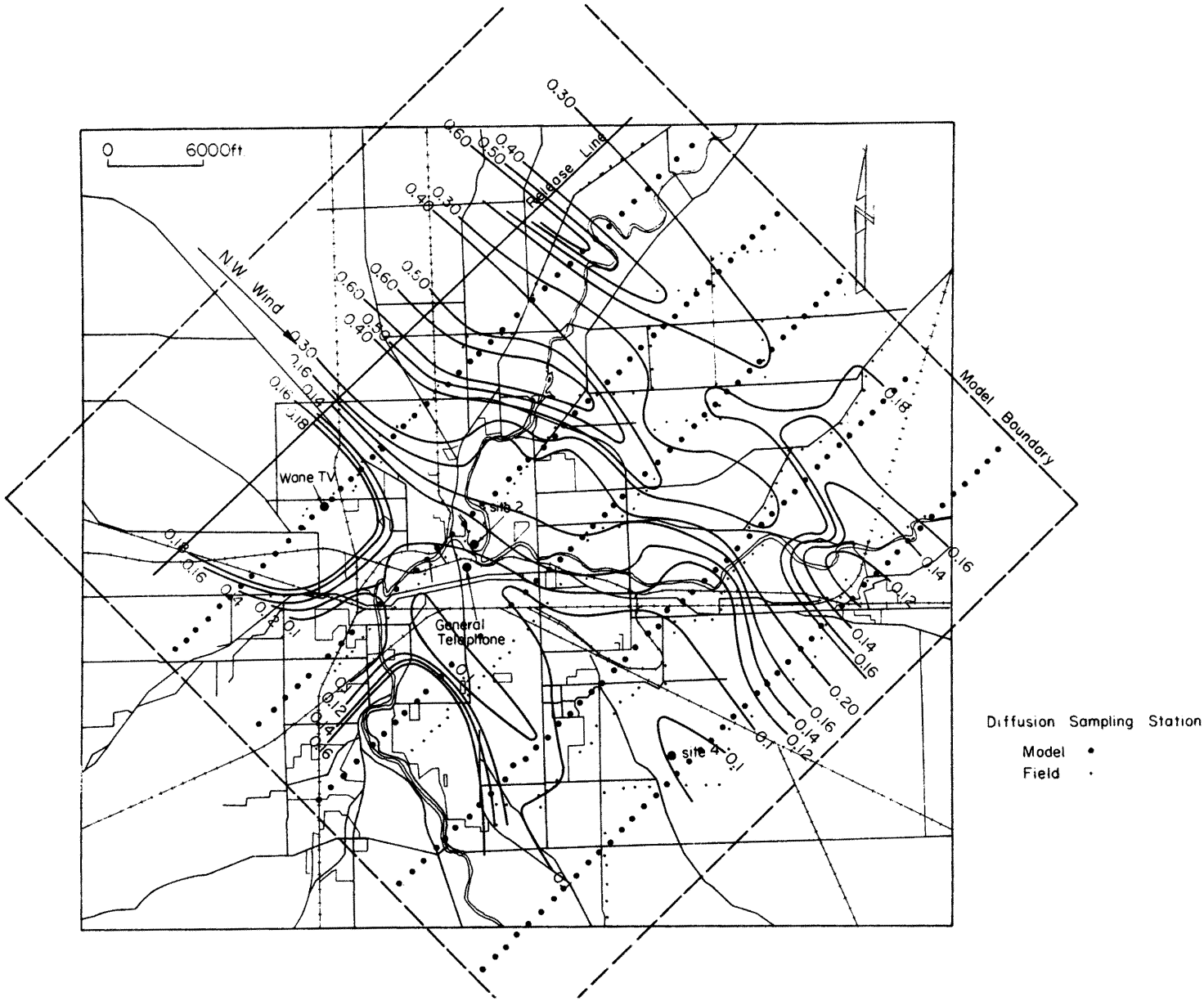

Figure 7. Model Lay-Out and Diffusion Sampling Stations

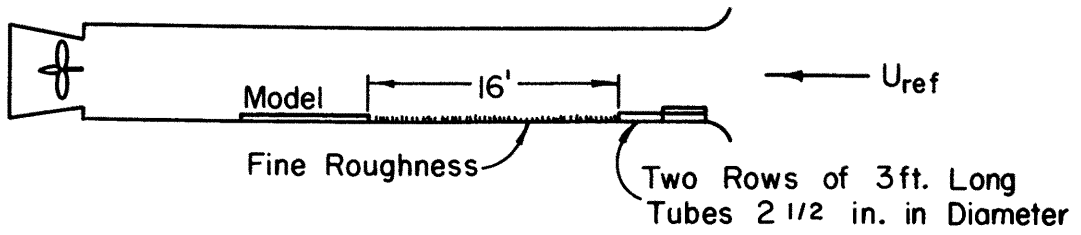

Velocity Profile Production Arrangement

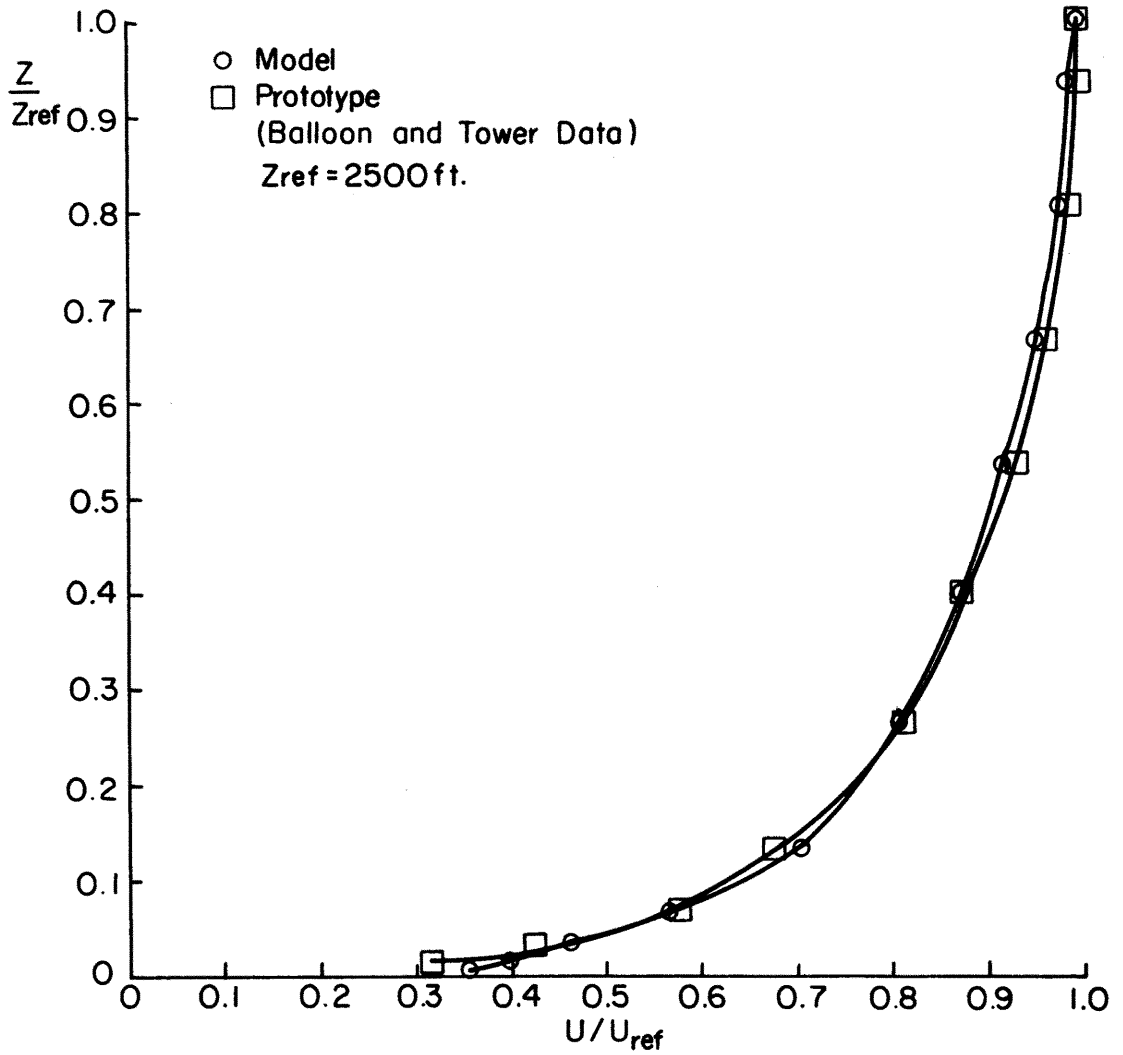

Figure 9. Comparison of Model and Prototype Velocity Profiles Approaching the City

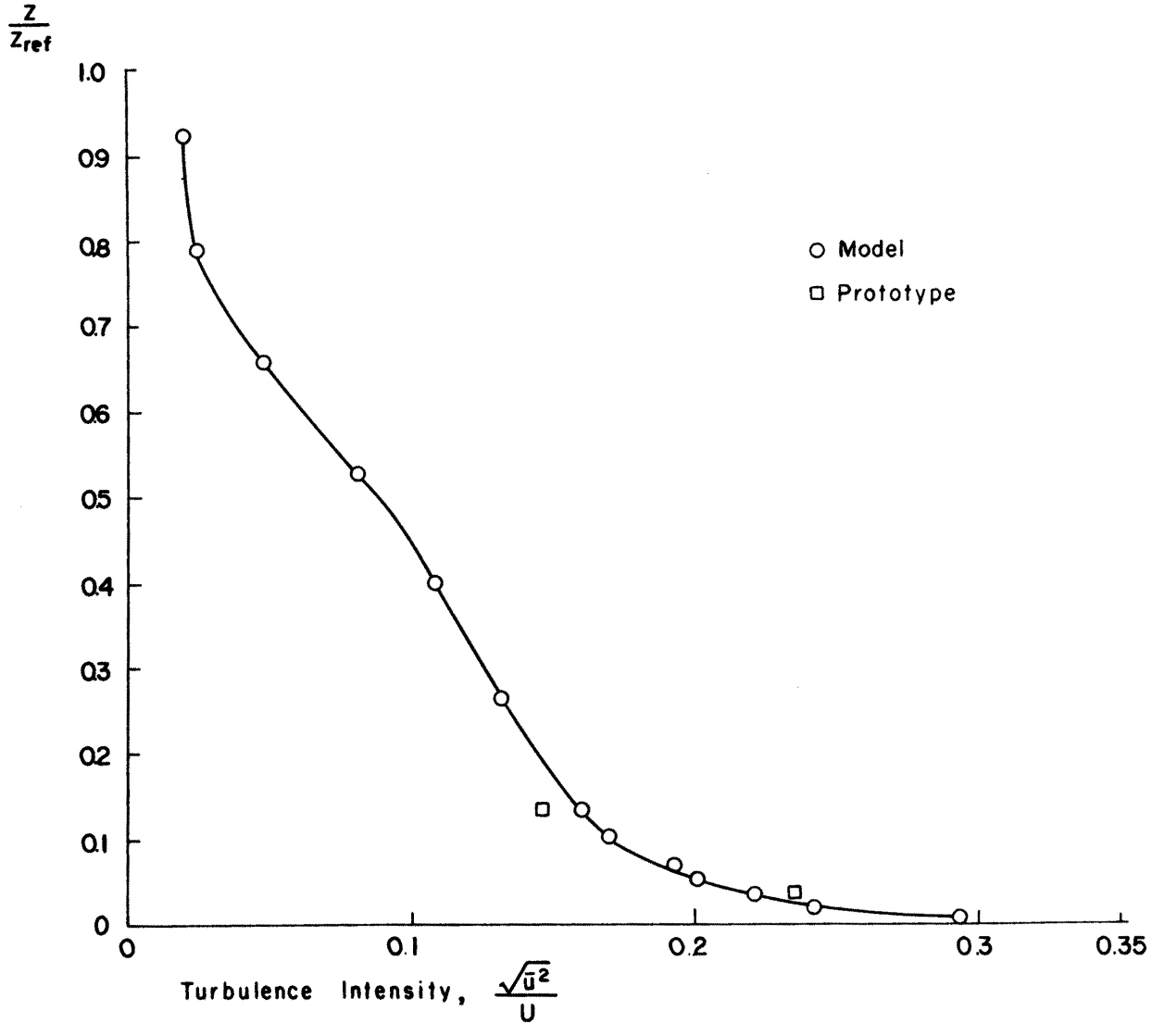

Figure 10. Comparison of Model and Prototype Turbulence Intensities

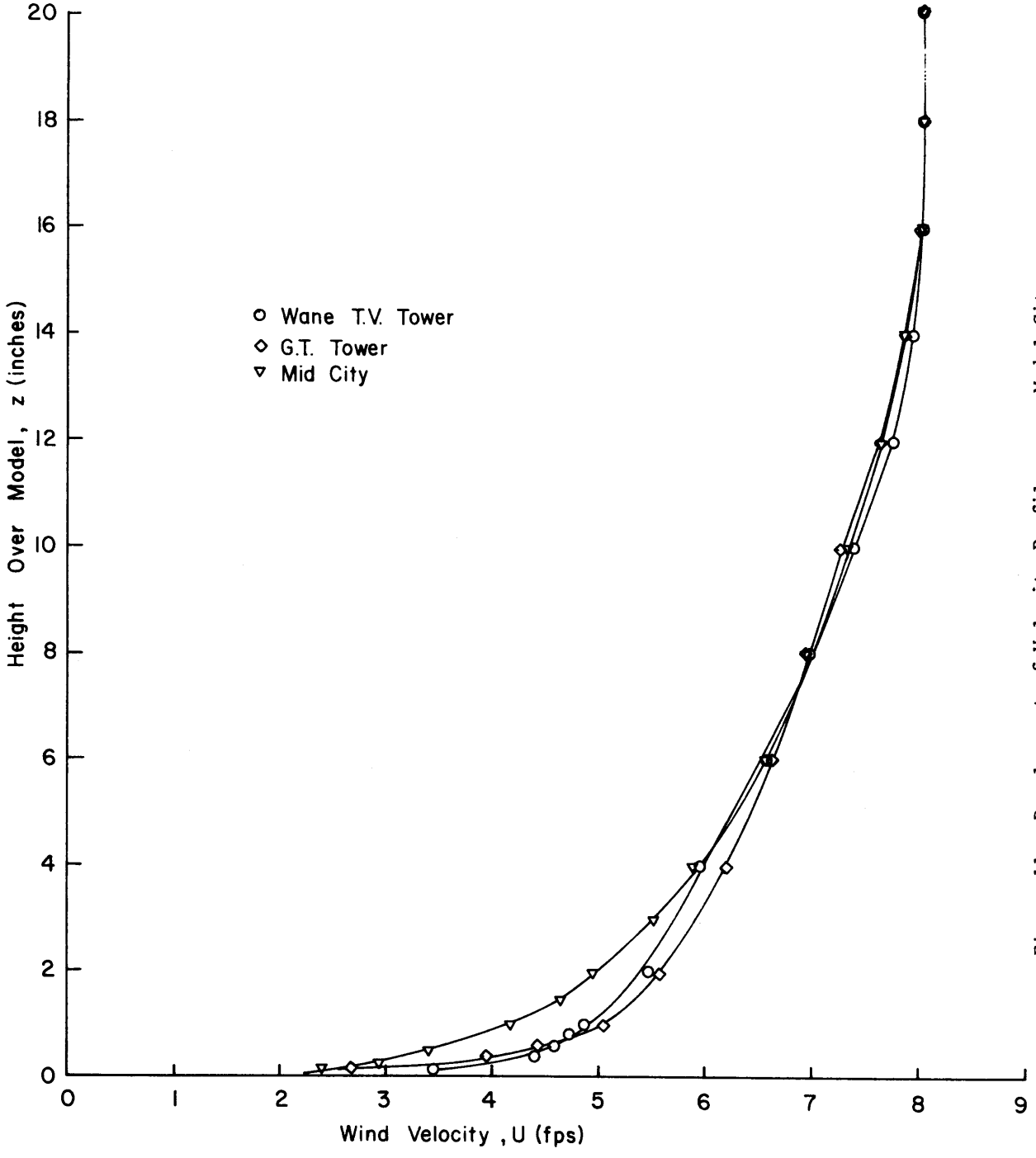

Figure 11. Development of Velocity Profiles over Model City

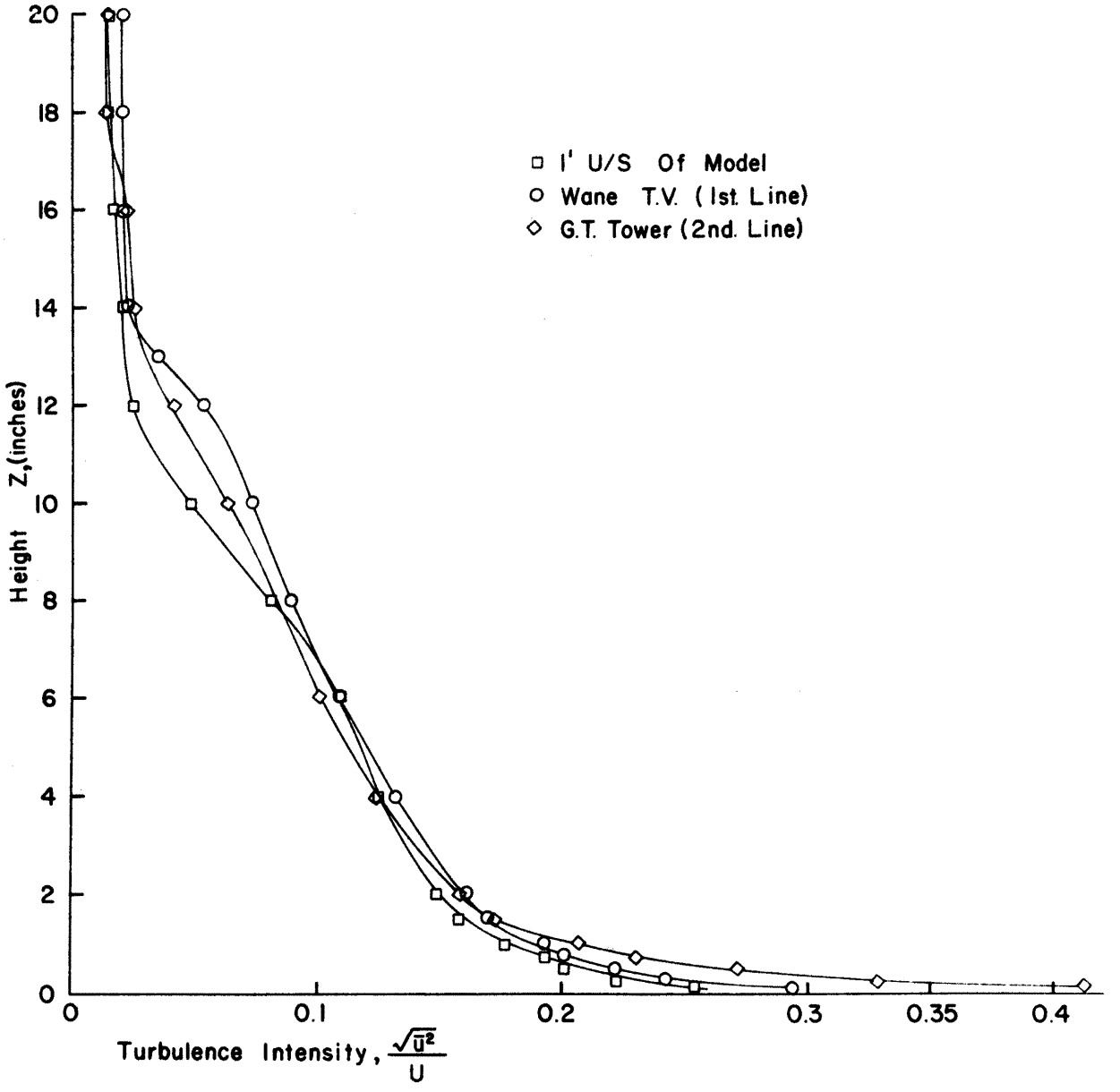

Figure 12. Development of Turbulence Intensity Profiles over the Model City

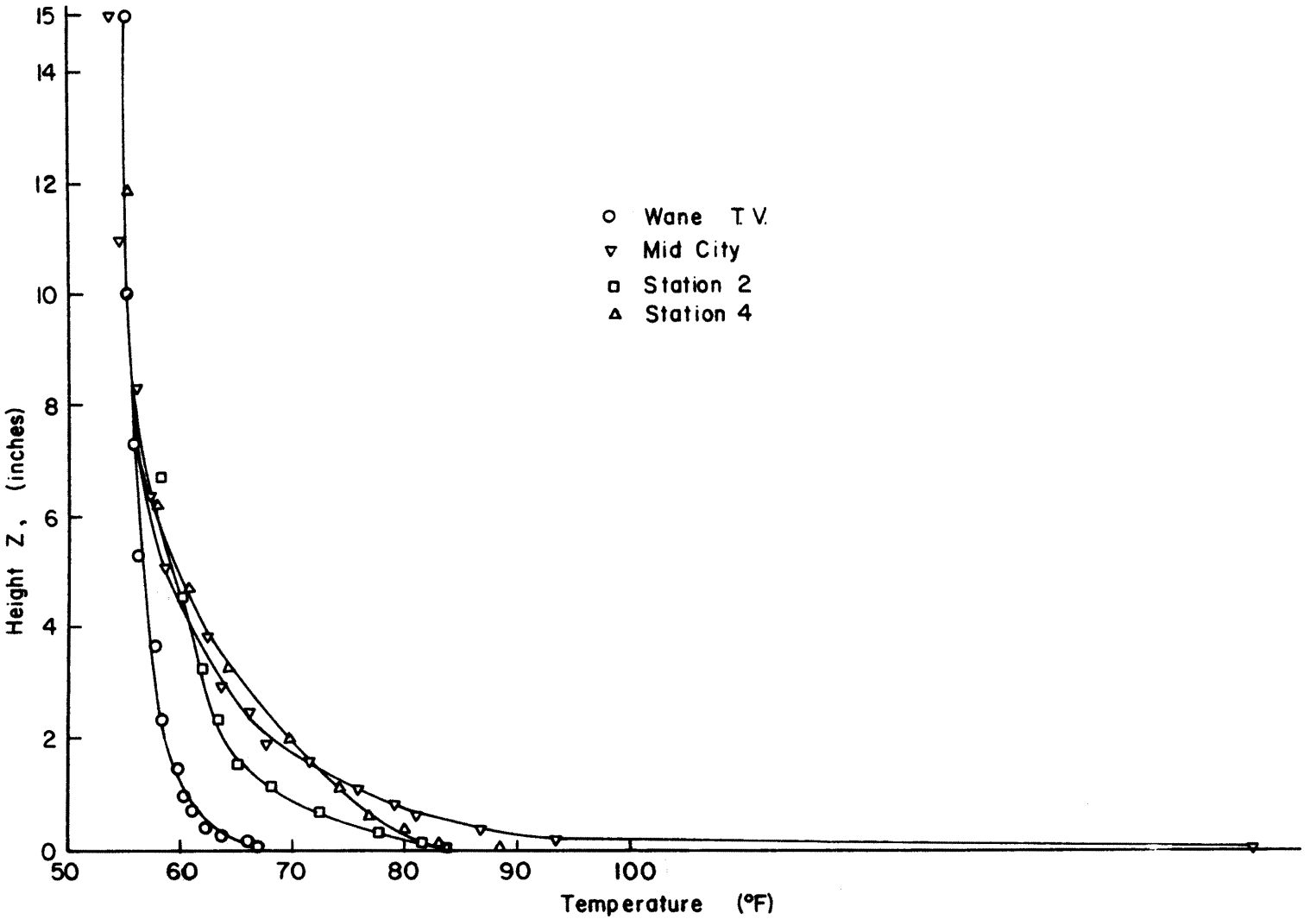

Figure 13. Development of Temperature Profiles over the Model City

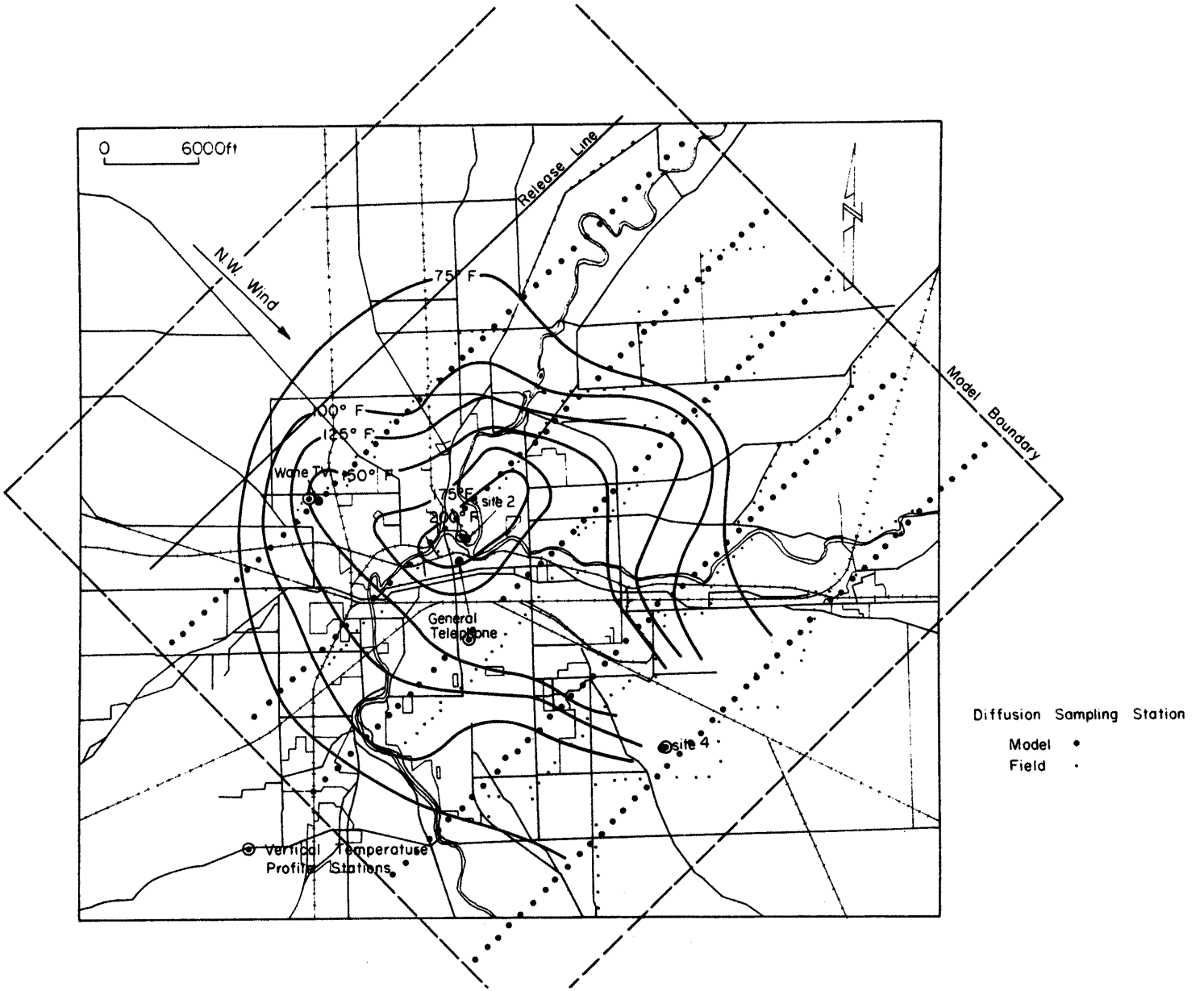

Figure 14. "Heat Island" Generated Over the Model City

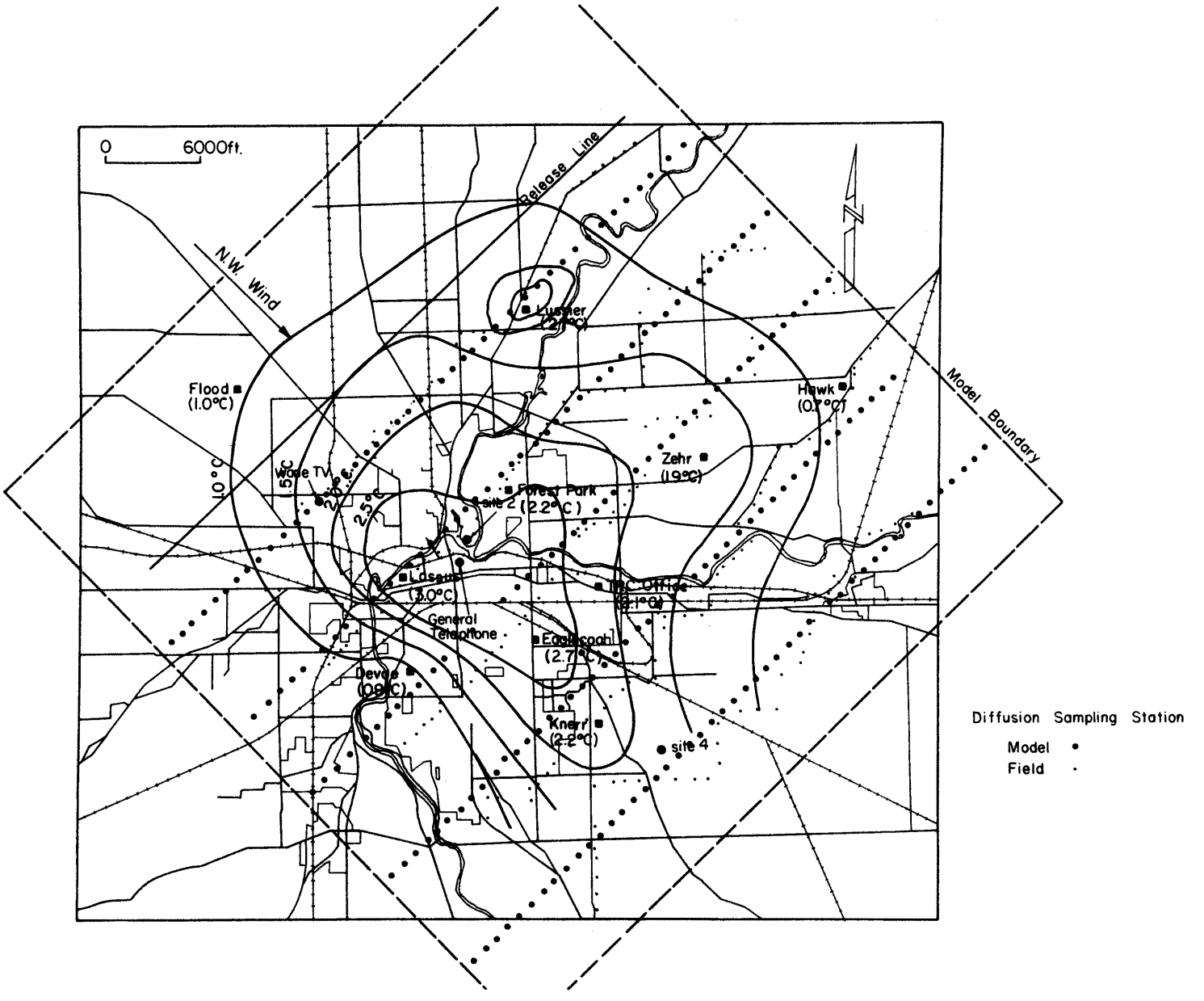

Figure 15. "Heat Island" Observed over Fort Wayne

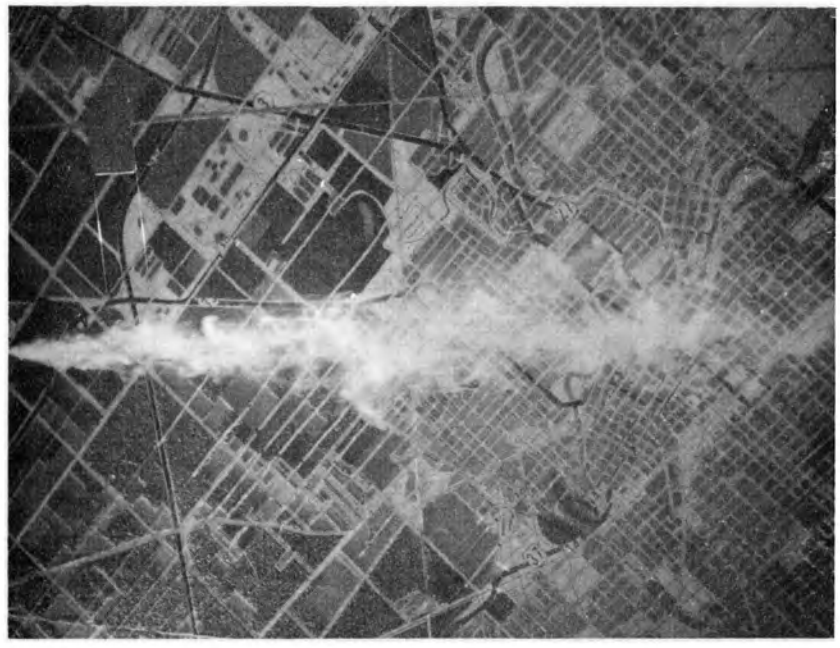

A. Plan View

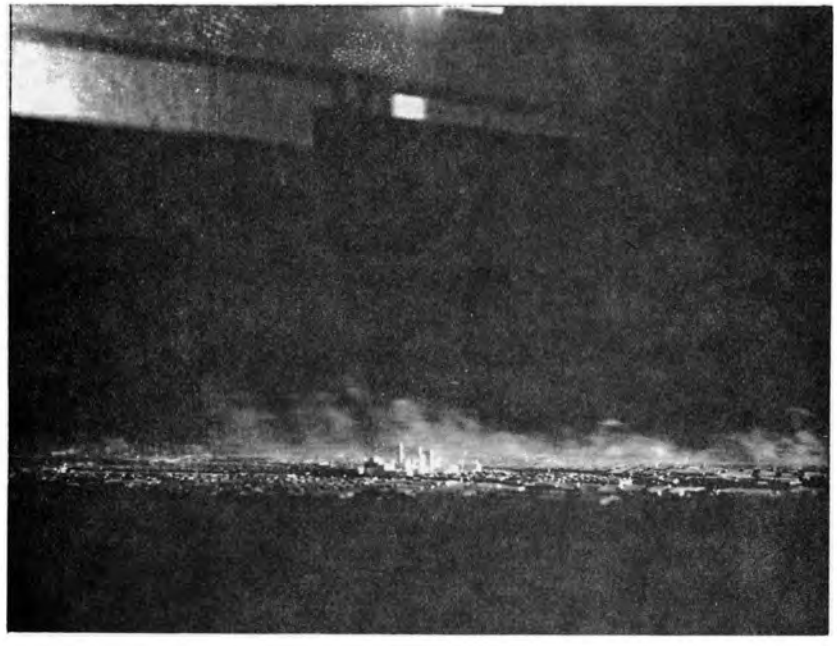

B. Side View

Figure 16 Smoke Diffusion over the Model

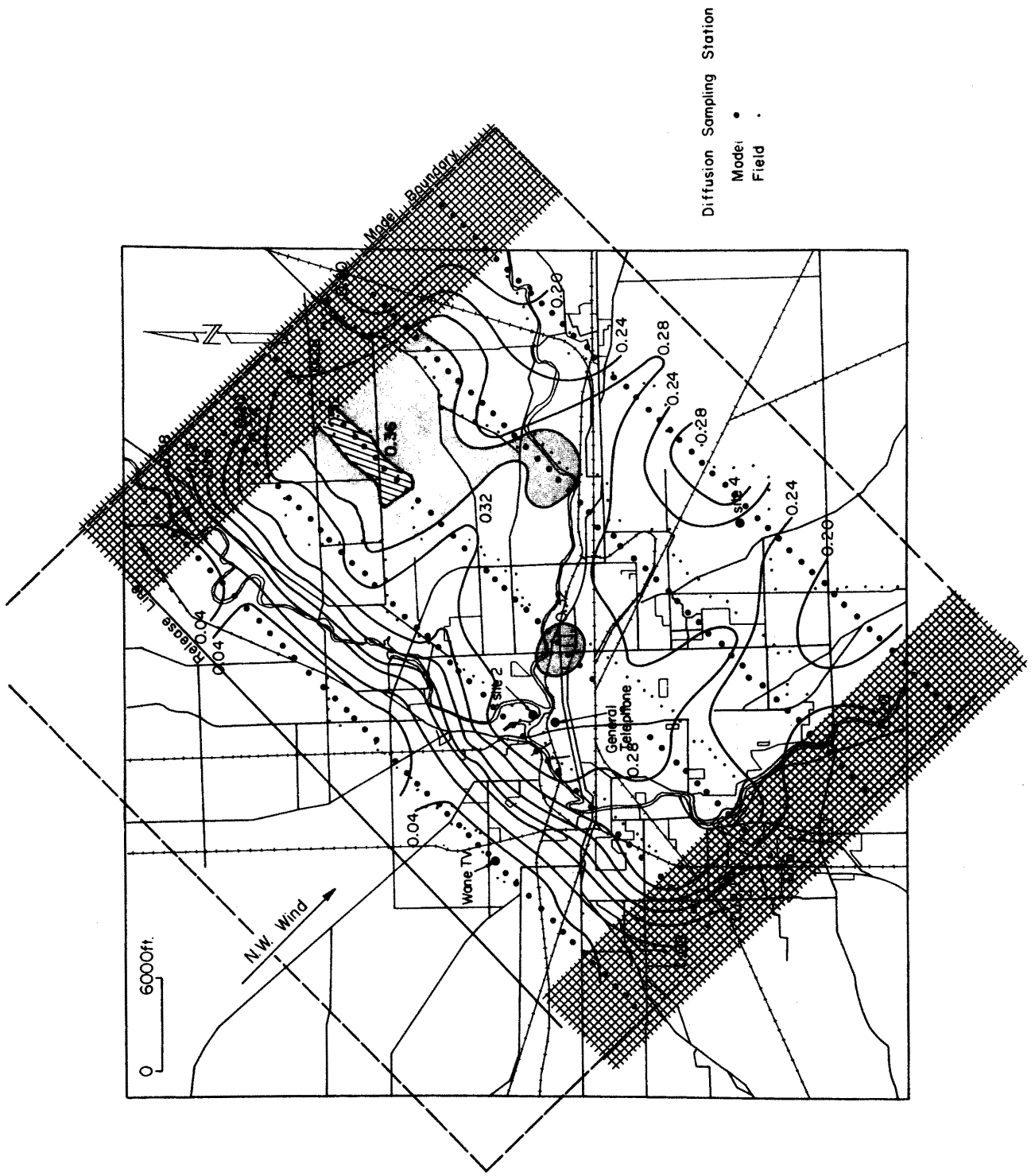

Figure 17. Surface Dosage Pattern Observed over the Model. The Numbers on the Iso-Dosage Lines Indicate Non-Dimensional Dosage Defined on Page 28.

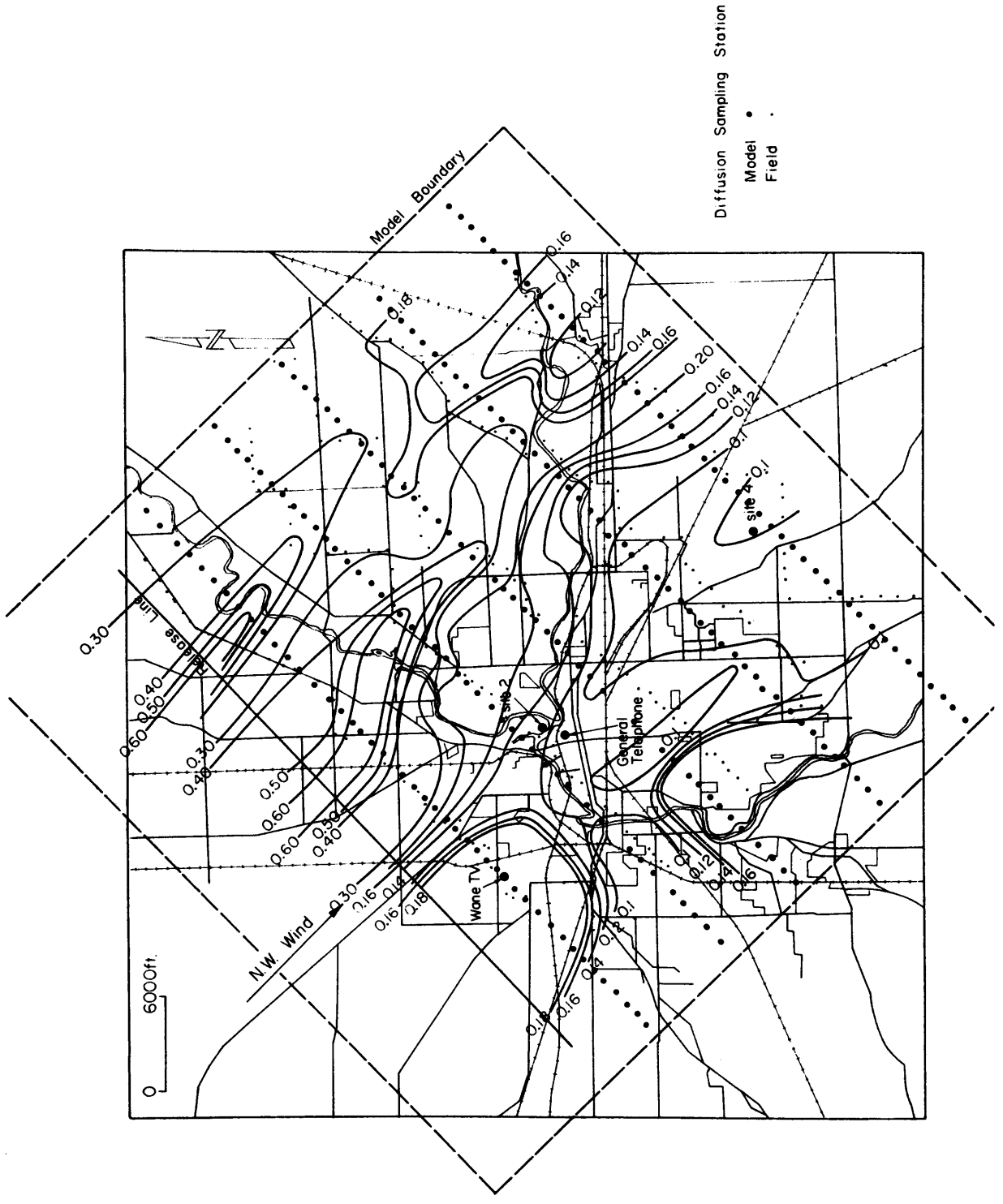

Figure 18. Surface Dosage Pattern Observed In Fort Wayne During Trial 65-06-G2. The Numbers on the Iso-Dosage Lines Indicate Non-Dimensional Dosage Defined on Page 28.

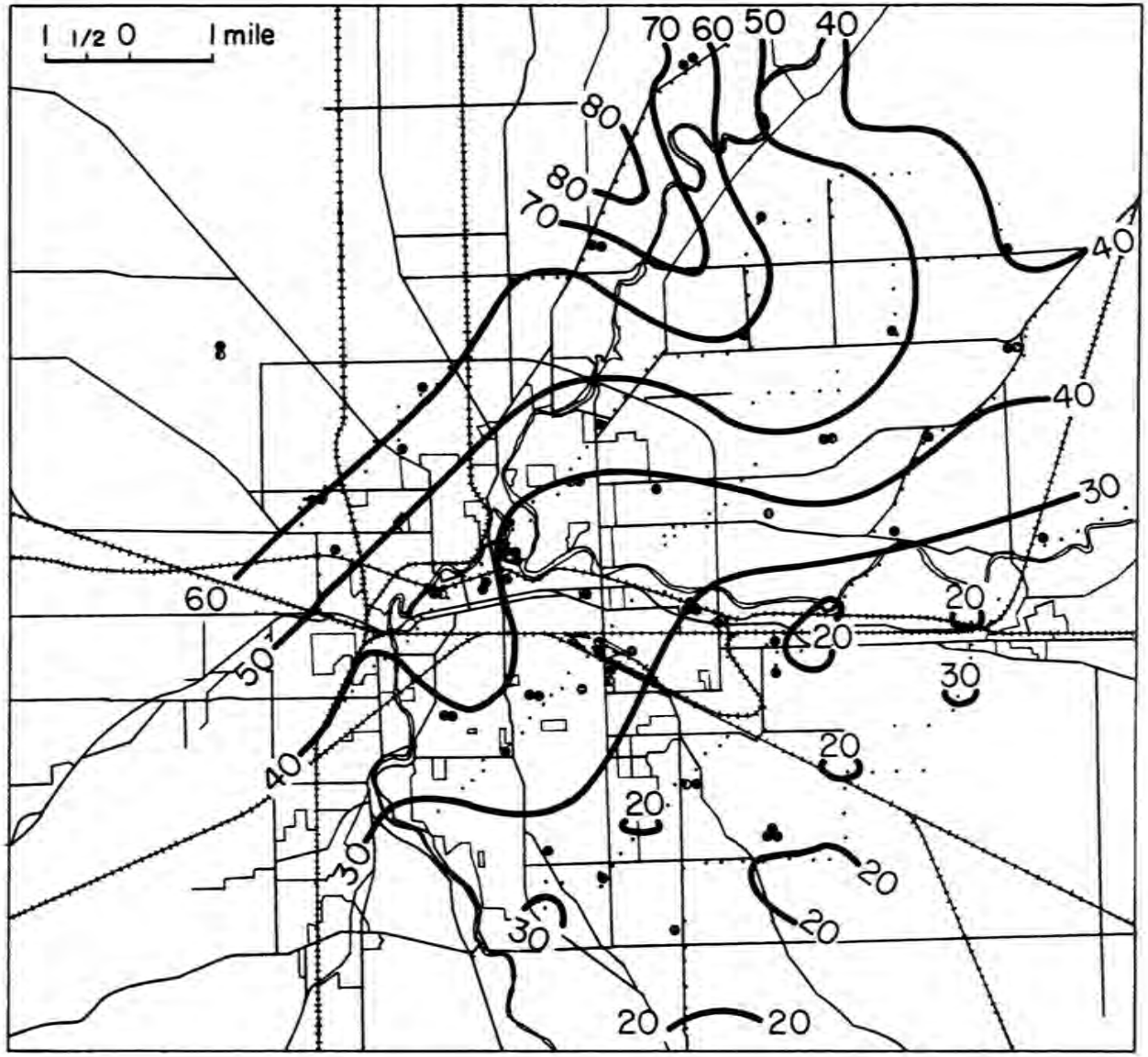

Figure 19. Average Surface Dosage Observed in Fort Wayne City and Rural Areas During 70 Trials, in Particle-Min/Liter (After Hilst and Bowne 1966)

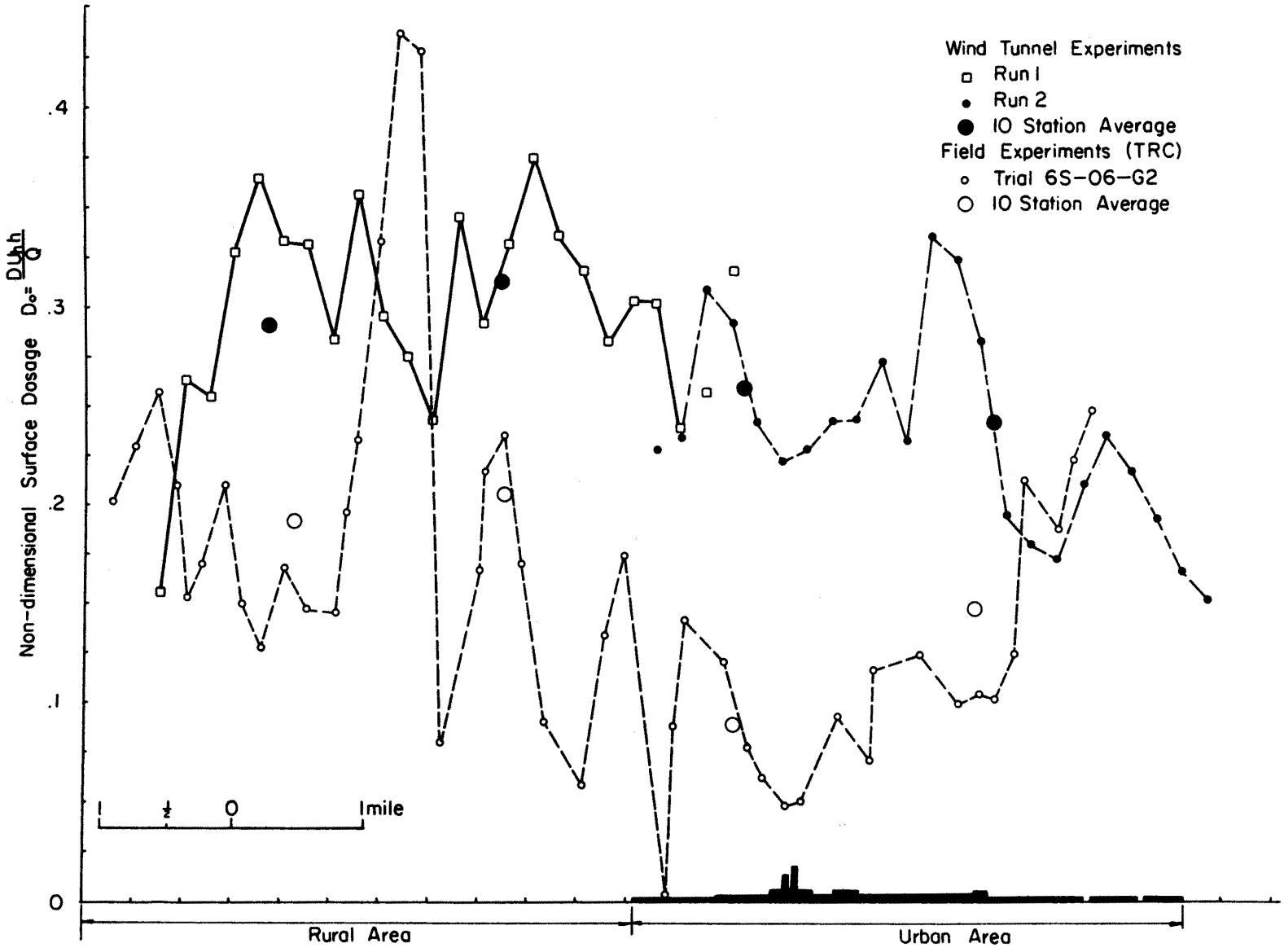

Figure 20. Comparison of Model and Field Surface Dosages at 7 Mile Distance from Release Line

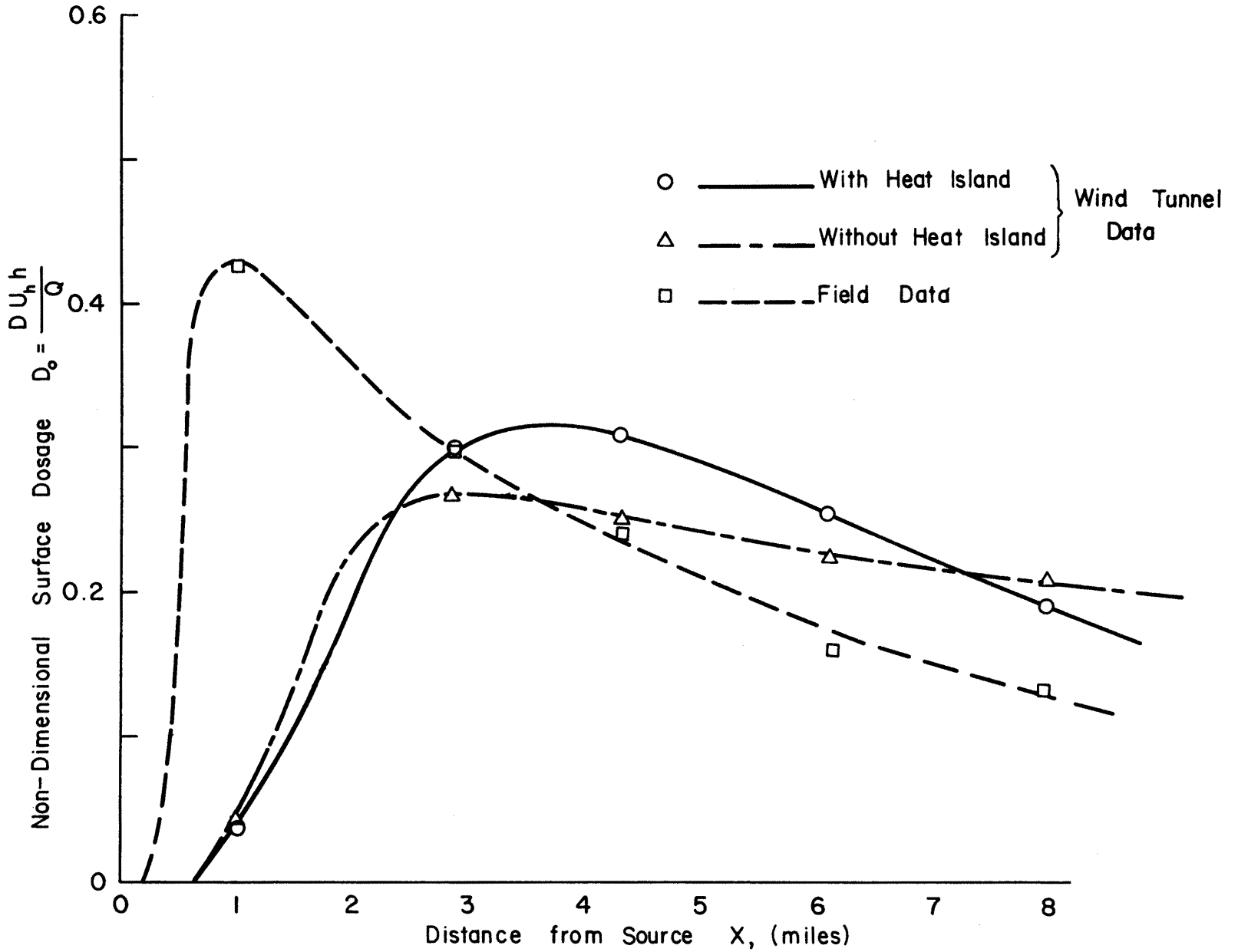

Figure 21. Longitudinal Variation of Surface Dosages over the Model City and the Prototype

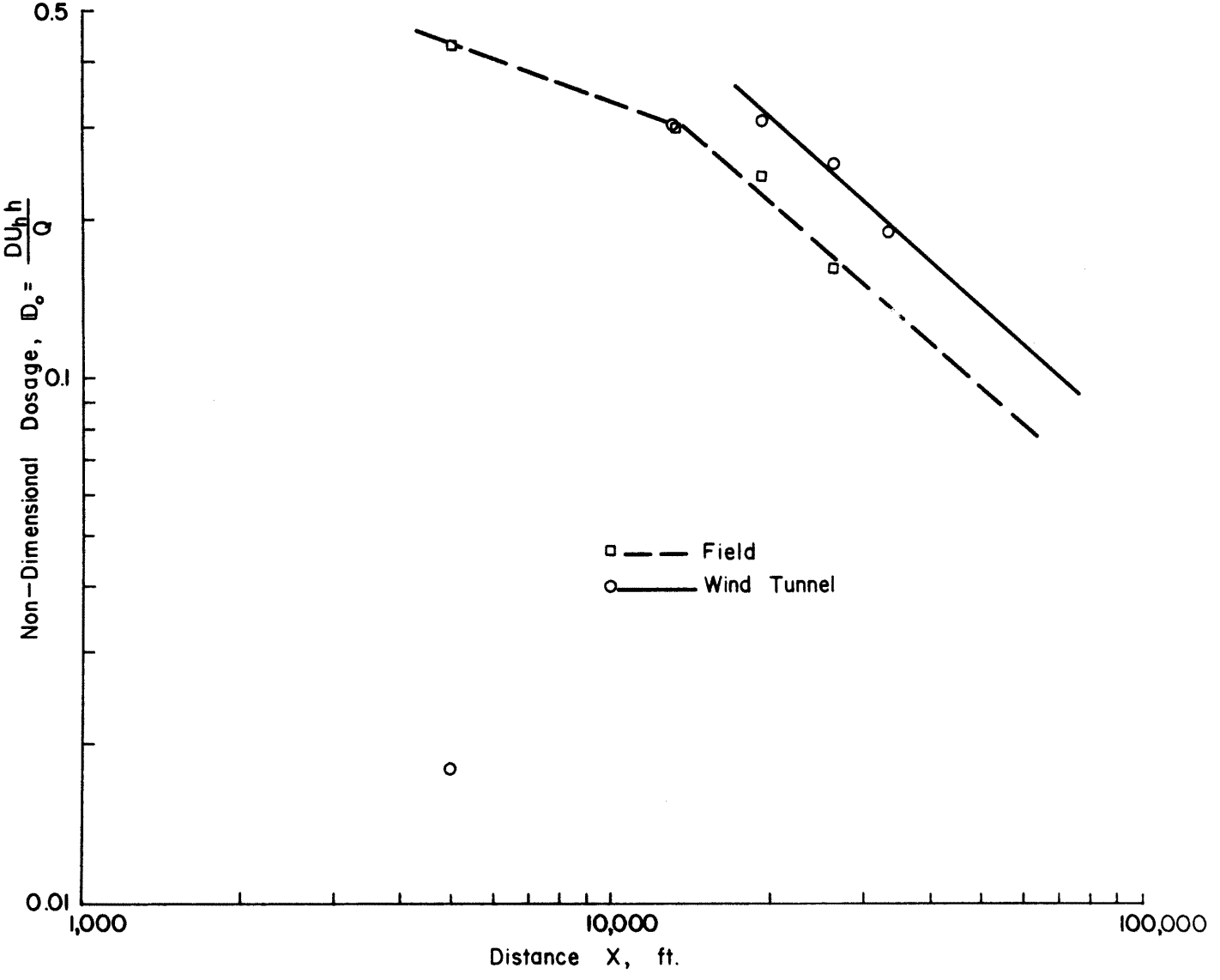

Figure 22. Comparison of Rate of Decrease of Surface Dosage with Distance Observed over the Model and Prototype

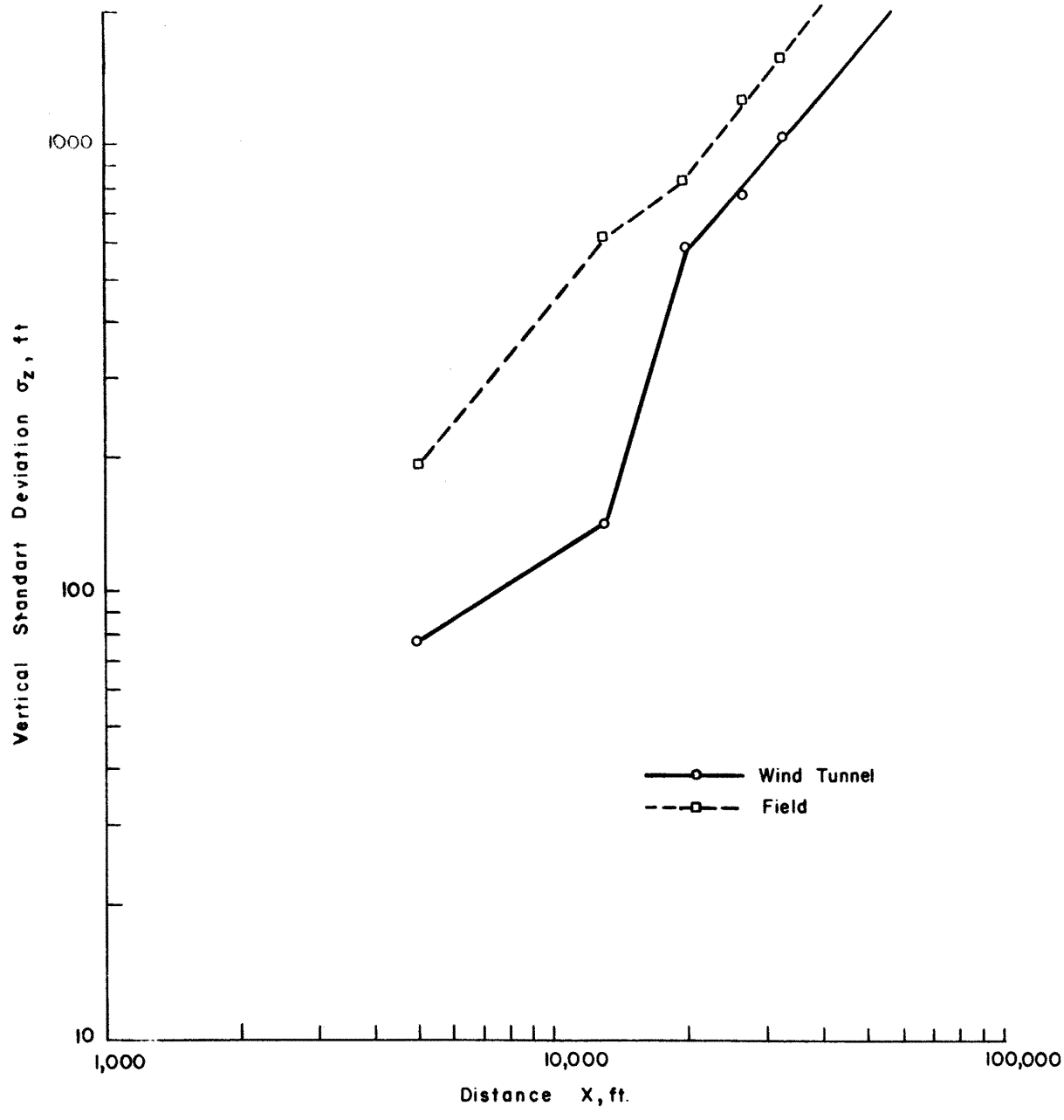

Figure 23. Comparison of Field and Wind Tunnel Rates of Vertical Growth of the Cloud

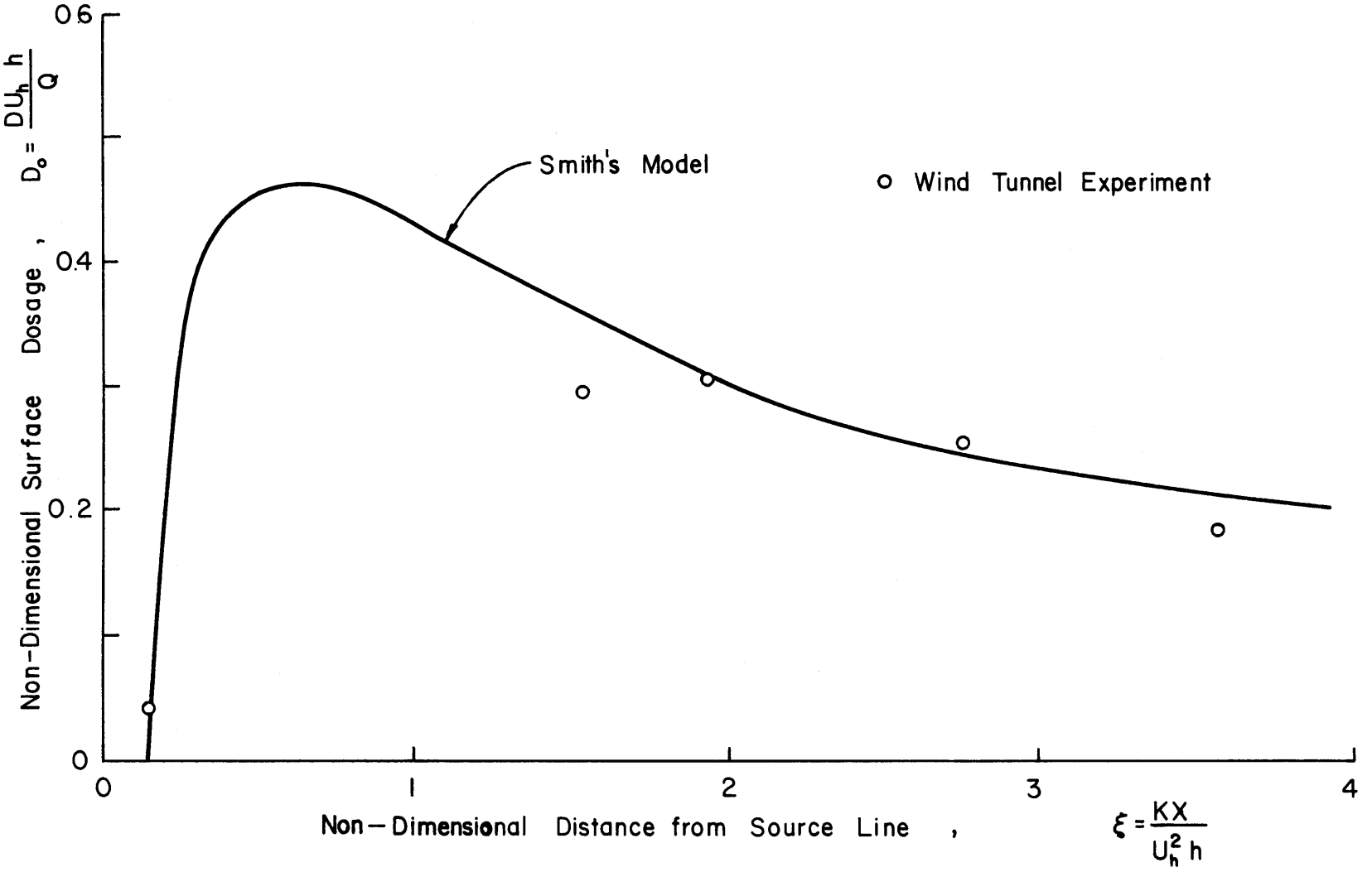

Figure 24. Comparison of Surface Dosages Observed over the Model with those Predicted from Smith's Theory

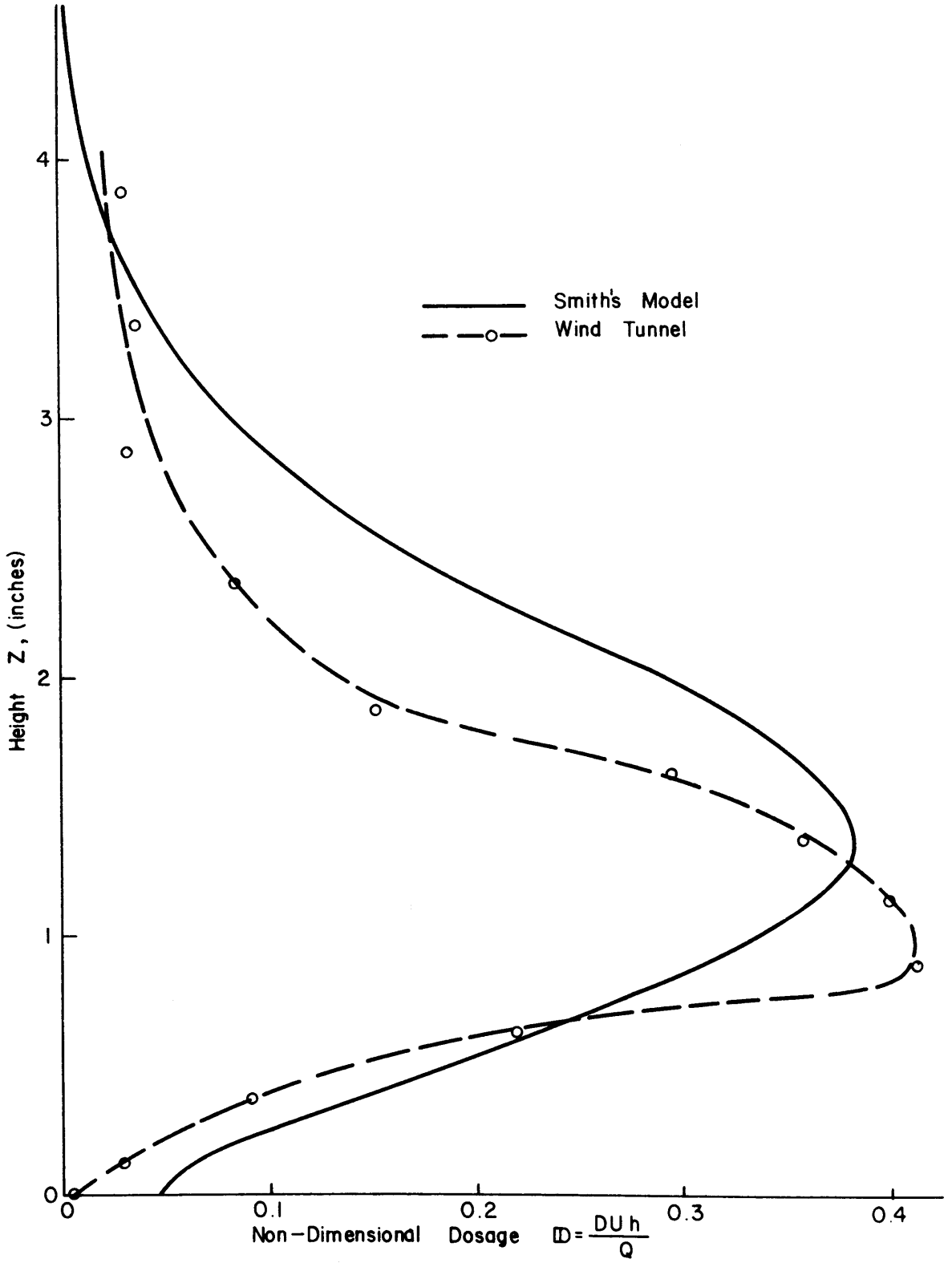

Figure 25. Comparison of Vertical Dosage Profile Observed at the First Sampling Line in the Model with Smith's Theory.

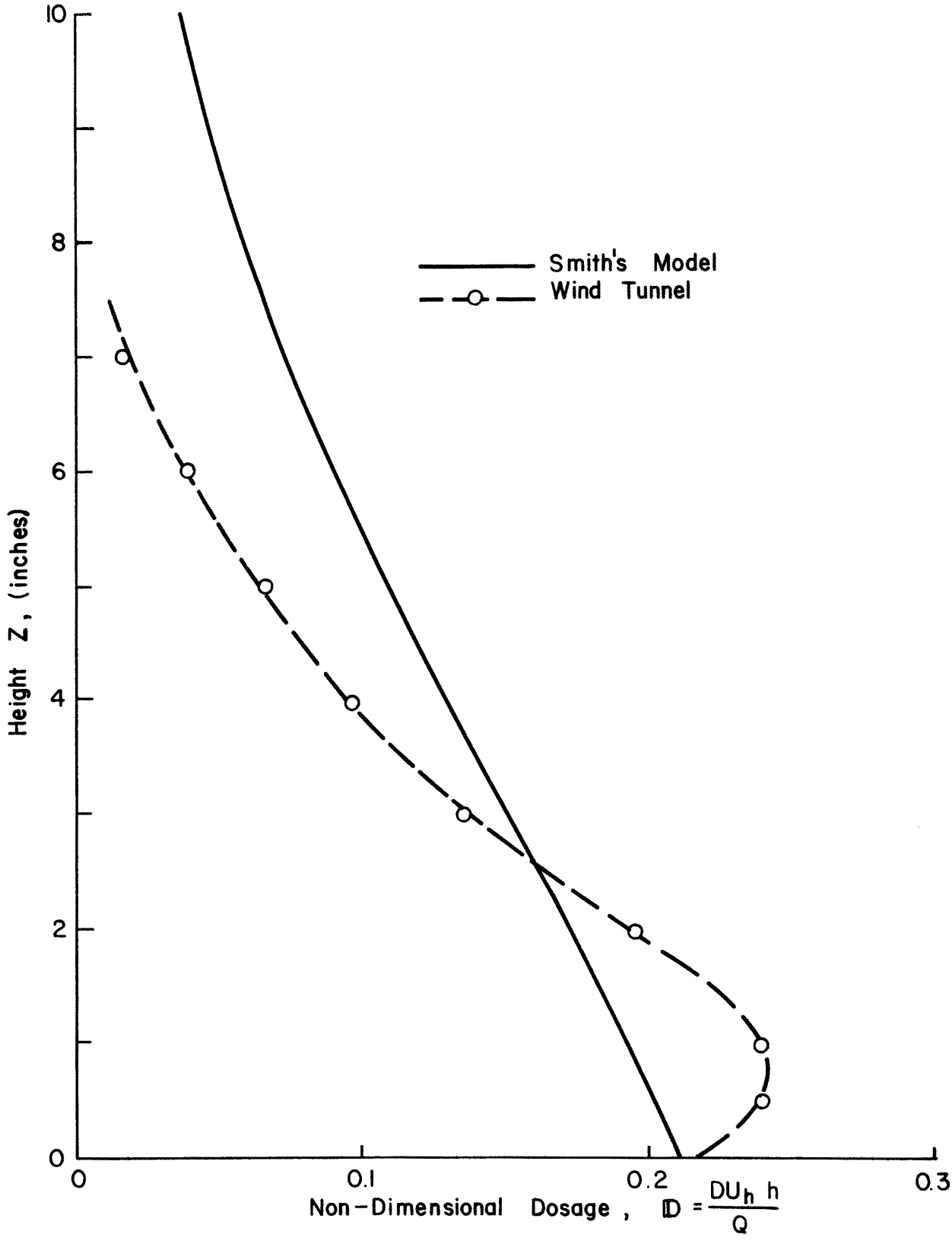

Figure 26. Comparison of Vertical Dosage Profile Observed at the Last Sampling Line in the Model with Smith's Theory

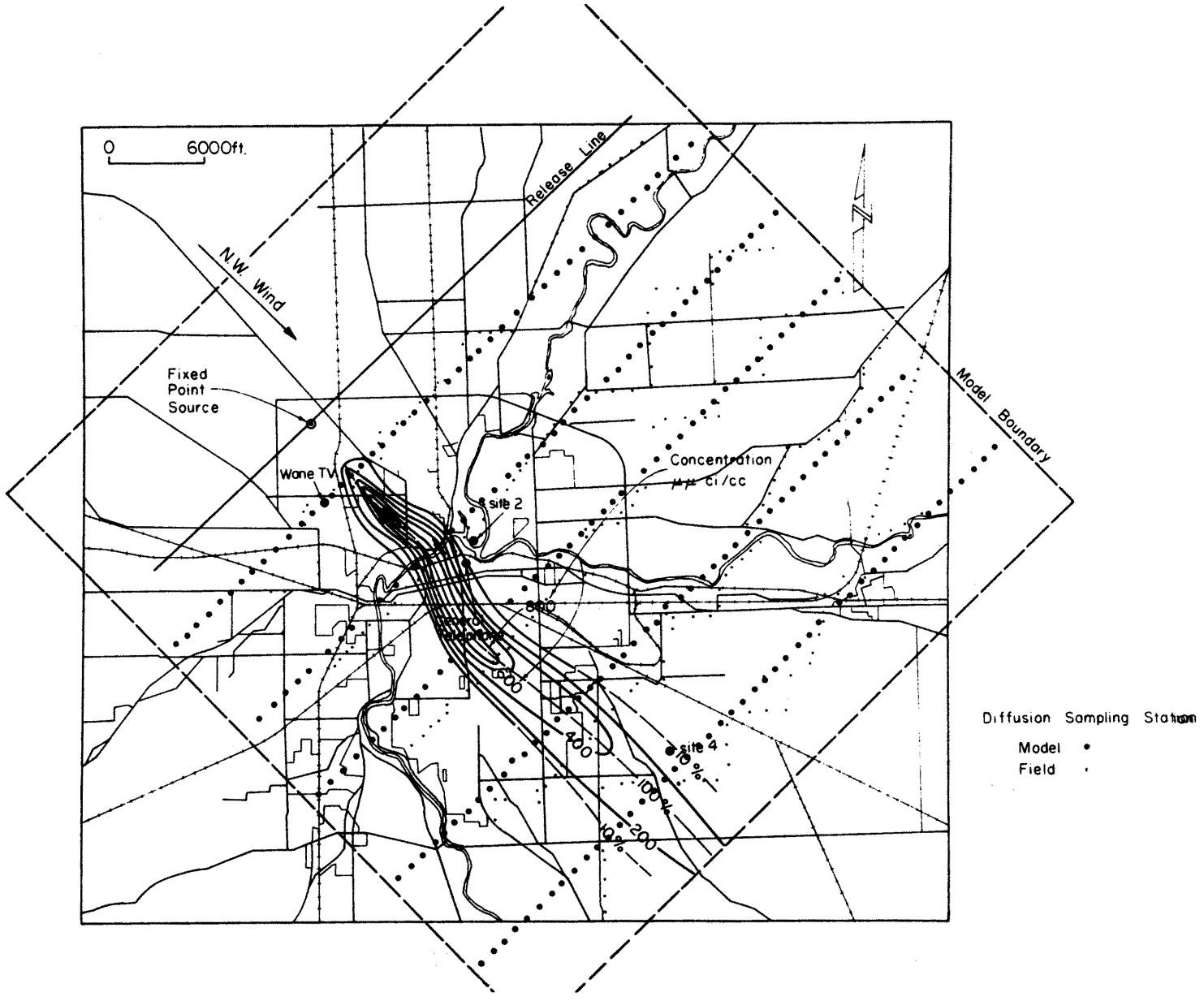

Figure 27. Surface Concentration Pattern due to the Fixed Elevated Continuous Source placed Upwind from the City Model.

Unclassified
Security Classification

DOCUMENT CONTROL DATA - R & D

(Security classification of title, body of abstract and indexing annotation must be entered when the overall report is classified)

1. ORIGINATING ACTIVITY *(Corporate author)*
Fluid Dynamics and Diffusion Laboratory
Engineering Research Center, Colorado State Univ.
Fort Collins, Colorado 80521

2a. REPORT SECURITY CLASSIFICATION
Unclassified

2b. GROUP

3. REPORT TITLE
"Wind Tunnel Modeling of Flow and Diffusion Over an Urban Complex"

4. DESCRIPTIVE NOTES *(Type of report and inclusive dates)*
THEMIS Technical Report No. 17

5. AUTHOR(S) *(First name, middle initial, last name)*
Chaudhry, F. H. and Cermak, J. E.

6. REPORT DATE	7a. TOTAL NO. OF PAGES	7b. NO. OF REFS
September 1969		27

8a. CONTRACT OR GRANT NO.	9a. ORIGINATOR'S REPORT NUMBER(S)
N00014-68-A-0493-0001	CER70-71FHC-JEC24
b. PROJECT NO. NR 062-414/6-6-68 (Code 438)	9b. OTHER REPORT NO(S) *(Any other numbers that may be assigned this report)*
c.	
d.	

10. DISTRIBUTION STATEMENT
Distribution of this report is unlimited

11. SUPPLEMENTARY NOTES	12. SPONSORING MILITARY ACTIVITY
	Office of Naval Research

13. ABSTRACT

The purpose of this study is to explore and test the powerful potential of wind-tunnel modeling as an alternative to the more expensive and tedious full-scale urban diffusion experiments.

A model of the city of Fort Wayne was constructed to a horizontal scale of 1: 4000 and studied in the environmental wind tunnel of the Fluid Dynamics and Diffusion Laboratory at Colorado State University. If the roughness and the heat-island effects are modelled properly, and the approach flows made similar, the flow over the model city was found to conform to that in the field. The pattern of the heat island over Fort Wayne is reproduced almost exactly in the model. Simulation of diffusion from an aerial line source was accomplished by traversing a continuously emitting source of Krypton-85 across the city. The measured dosages of this tracer over the city compare well with the corresponding field data except immediately downwind from the source where the downdraft from the disseminating aircraft becomes significant in the field. The model is found to give same overall picture of the effect of the city on dispersion process as that observed in the field. The results show that the heat island effect vitiates the environment by pulling pollutants down from elevated releases due to increased turbulence near the surface. The model results compare reasonably with approximate theory of Smith (1957).

The results of this study have proved that it is indeed possible to simulate the flow over a city and obtain useful information, relatively inexpensively, on urban diffusion.

DD FORM 1 NOV 65 1473

Unclassified
Security Classification

14 KEY WORDS	LINK A		LINK B		LINK C	
	ROLE	WT	ROLE	WT	ROLE	WT
Atmospheric Simulation						
Urban Diffusion Models						
Urban Planning						
Urban Atmosphere						
"Heat Island" effect						
Diffusion						
Air Pollution Meteorology						
Wind Tunnel Modeling						
Turbulent Boundary Layer						

April 1971

DISTRIBUTION LIST FOR UNCLASSIFIED
TECHNICAL REPORTS ISSUED UNDER
CONTRACT N00014-68-A TASK 000-414
0493-0001

Defense Documentation Center
Cameron Station
Alexandria, Virginia 22314 (12)

Technical Library
Naval Ship Research and Development Laboratory
Annapolis, Maryland 21402

Professor Bruce Johnson
Engineering Department
Naval Academy
Annapolis, Maryland 21402

Library
Naval Academy
Annapolis, Maryland 21402

Professor W.R. Debler
Department of Engineering Mechanics
University of Michigan
Ann Arbor, Michigan 48108

Professor W.P. Graebel
Department of Engineering Mechanics
University of Michigan
College of Engineering
Ann Arbor, Michigan 48108

Professor Finn C. Michelsen
Naval Architecture and Marine Engineering
445 West Engineering Building
University of Michigan
Ann Arbor, Michigan 48108

Dr. Francis Ogilvie
Department of Naval Architecture and Marine Engineering
University of Michigan
Ann Arbor, Michigan 48108

Professor W.W. Willmarth
Department of Aerospace Engineering
University of Michigan
Ann Arbor, Michigan 48108

Dr. S.A. Piacsek
Argonne National Laboratory
Applied Mathematics Division
9700 S. Cass Avenue
Argonne, Illinois 60439

AFOSR (REM)
1400 Wilson Boulevard
Arlington, Virginia 22204

Professor S. Corrsin
Mechanics Department
The Johns Hopkins University
Baltimore, Maryland 20910

Professor L.S.G. Kovasznay
The Johns Hopkins University
Baltimore, Maryland 20910

Professor O.M. Phillips
The Johns Hopkins University
Baltimore, Maryland 20910

Librarian
Department of Naval Architecture
University of California
Berkeley, California 94720

Professor Israel Cornet
Department of Mechanical Engineering
University of California
Berkeley, California 94720

Professor M. Holt
Division of Aeronautical Sciences
University of California
Berkeley, California 94720

Professor E.V. Laitone
Department of Mechanical Engineering
University of California
Berkeley, California 94720

Professor P. Lieber
Department of Mechanical Engineering
University of California
Institute of Engineering Research
Berkeley, California 94720

Professor J.R. Paulling
Department of Naval Architecture
University of California
Berkeley, California 94720

Professor J.V. Wehausen
Department of Naval Architecture
University of California
Berkeley, California 94720

Professor E.R. van Driest
Virginia Polytechnic Institute and University
Department of Aerospace Engineering
Blacksburg, Virginia 24061

Commander
Boston Naval Shipyard
Boston, Massachusetts 02129

Director
Office of Naval Research Branch Office
495 Summer Street
Boston, Massachusetts 02210

Commander
Puget Sound Naval Shipyard
Bremerton, Washington 98314

Professor J.J. Foody
Chairman, Engineering Department
State University of New York
Maritime College
Bronx, New York 10465

Dr. Alfred Ritter
Assistant Head, Applied Mechanics Department
Cornell Aeronautical Laboratory, Inc.
Buffalo, New York 14221

Dr. J.W. Morris
Manager, Material Sciences Section
Advanced Materials Research
Bell Aerospace Company
P.O. Box 1
Buffalo, New York 14240

Professor G.H. Carrier
Department of Engineering and Applied Physics
Harvard University
Cambridge, Massachusetts 02138

Commanding Officer
NROTC Naval Administrative Unit
Massachusetts Institute of Technology
Cambridge, Massachusetts 02139

Professor M.A. Abkowitz
Department of Naval Architecture and Marine Engineering
Massachusetts Institute of Technology
Cambridge, Massachusetts 02139

Professor A.T. Ippen
Department of Civil Engineering
Massachusetts Institute of Technology
Cambridge, Massachusetts 02139

Professor L.N. Howard
Department of Mathematics
Massachusetts Institute of Technology
Cambridge, Massachusetts 02139

Professor E.W. Merrill
Department of Mathematics
Massachusetts Institute of Technology
Cambridge, Massachusetts 02139

Professor E. Mollo-Christensen
Room 54-1722
Massachusetts Institute of Technology
Cambridge, Massachusetts 02139

Professor N. Newman
Department of Naval Architecture and Marine Engineering
Massachusetts Institute of Technology
Cambridge, Massachusetts 02139

Professor A.H. Shapiro
Department of Mechanical Engineering
Massachusetts Institute of Technology
Cambridge, Massachusetts 02139

Commander
Charleston Naval Shipyard
U.S. Naval Base
Charleston, South Carolina 29408

A.R. Kuhlthau, Director
Research Laboratories for the Engineering Sciences
Thorton Hall, University of Virginia
Charlottesville, Virginia 22903

Director
Office of Naval Research Branch Office
536 South Clark Street
Chicago, Illinois 60605

Library
Naval Weapons Center
China Lake, California 93555

Professor J.M. Burgers
Institute of Fluid Dynamics and Applied Mathematics
University of Maryland
College Park, Maryland 20742

Professor Pai
Institute for Fluid Dynamics and Applied Mathematics
University of Maryland
College Park, Maryland 20740

Acquisition Director
NASA Scientific & Technical Information
P.O. Box 33
College Park, Maryland 20740

Technical Library
Naval Weapons Laboratory
Dahlgren, Virginia 22448

Computation & Analyses Laboratory
Naval Weapons Laboratory
Dahlgren, Virginia 22448

Dr. C.S. Wells, Jr.
Manager - Fluid Mechanics
Advanced Technology Center, Inc.
P.O. Box 6144
Dallas, Texas 75222

Dr. R.H. Kraichnan
Dublin, New Hampshire 03444

Commanding Officer
Army Research Office
Box CM, Duke Station
Durham, North Carolina 27706

Professor A. Charnes
The Technological Institute
Northwestern University
Evanston, Illinois 60201

Dr. Martin H. Bloom
Polytechnic Institute of Brooklyn
Graduate Center, Dept. of Aerospace
Engineering and Applied Mechanics
Farmingdale, New York 11735

Technical Documents Center
Building 315
U.S. Army Mobility Equipment
Research and Development Center
Fort Belvoir, Virginia 22060

Professor J.E. Cermak
College of Engineering
Colorado State University
Ft. Collins, Colorado 80521

Technical Library
Webb Institute of Naval Architecture
Glen Cove, Long Island, New York 11542

Professor E.V. Lewis
Webb Institute of Naval Architecture
Glen Cove, Long Island, New York 11542

Dr. B.N. Pridmore Brown
Northrop Corporation
NORAIR-Div.
Hawthorne, California 90250

Dr. J.P. Breslin
Stevens Institute of Technology
Davidson Laboratory
Hoboken, New Jersey 07030

Dr. D. Savitsky
Stevens Institute of Technology
Davidson Laboratory
Hoboken, New Jersey 07030

Mr. C.H. Henry
Stevens Institute of Technology
Davidson Laboratory
Hoboken, New Jersey 07030

Dr. J.P. Craven
University of Hawaii
1801 University Avenue
Honolulu, Hawaii 96822

Professor E.L. Resler
Graduate School of Aeronautical Engineering
Cornell University
Ithaca, New York 14851

Professor John Miles
c/o I.G.P.P.
University of California, San Diego
La Jolla, California 92038

Director
Scrippe Institution of Oceanography
University of California
La Jolla, California 92037

Professor A. Ellis
University of California, San Diego
Department of Aerospace & Mechanical Engineering
La Jolla, California 92037

Dr. B. Sternlicht
Mechanical Technology Incorporated
968 Albany-Shaker Road
Latham, New York 12110

Dr. Coda Pan
Mechanical Technology Incorporated
968 Albany-Shaker Road
Latham, New York 12110

Mr. P. Eisenberg, President
Hydronautics, Inc.
Pindell School Road
Howard County
Laurel, Maryland 20810

Mr. M.P. Tulin
Hydronautics, Inc.
Pindell School Road
Howard County
Laurel, Maryland 20810

Mr. Alfonso Alcedan L.,Director
Laboratorio Nacional De Hydraulics
Antigui Cameno A. Ancon
Casilla Jostal 682
Lima, Peru

Commander
Long Beach Naval Shipyard
Long Beach, California 90802

Professor John Laufer
Department of Aerospace Engineering
University Park
Los Angeles, California 90007

Professor J.M. Killen
St. Anthony Falls Hydraulic Lab.
University of Minnesota
Minneapolis, Minnesota 55414

Lorenz G. Straub Library
St. Anthony Falls Hydraulic Lab.
Mississippi River at 3rd Avenue S.E.
Minneapolis, Minnesota 55414

Professor J. Ripkin
St. Anthony Falls Hydraulic Lab.
University of Minnesota
Minneapolis, Minnesota 55414

Dr. W. Silberman
St. Anthony Falls Hydraulic Lab.
Mississippi River at 3rd Avenue S.E.
Minneapolis, Minnesota 55414

Superintendent
Naval Postgraduate School
Library Code 0212
Monterey, California 93940

Professor A.B. Metzner
University of Delaware
Newark, New Jersey 19711

Technical Library
Naval Underwater Systems Center
Newport, Rhode Island 02840

Professor Dudley D. Fuller
Department of Mechanical Engineering
Columbia University
New York, New York 10027

Professor V. Castelli
Department of Mechanical Engineering
Columbia University
New York, New York 10027

Professor H. Elrod
Department of Mechanical Engineering
Columbia University
New York, New York 10027

Professor J.J. Stoker
Institute of Mathematical Sciences
New York University
251 Mercer Street
New York, New York 10003

Society of Naval Architects and Marine Engineering
74 Trinity Place
New York, New York 10006

Engineering Societies Library
345 East 47th Street
New York, New York 10017

Office of Naval Research
New York Area Office
207 W. 24th Street
New York, New York 10011

Miss O.M. Leach, Librarian
National Research Council
Aeronautical Library
Montreal Road
Ottawa 7, Canada

Technical Library
Naval Ship Research and Development Center
Panama City, Florida 32401

Technical Library
Naval Undersea R & D Center
Pasadena Laboratory
3202 E. Foothill Boulevard
Pasadena, California 91107

Dr. Andrew Fabula
Naval Undersea Research & Development Center
Pasadena Laboratory
3202 E. Foothill Boulevard
Pasadena, California 91107

Dr. J.W. Hoyt
Naval Undersea R & D Center
Pasadena Laboratory
3202 E. Foothill Boulevard
Pasadena, California 91107

Professor A. Acosta
Department of Mechanical Engineering
California Institute of Technology
Pasadena, California 91109

Professor H. Liepmann
Department of Aeronautics
California Institute of Technology
Pasadena, California 91109

Professor M.S. Plesset
Engineering Division
California Institute of Technology
Pasadena, California 91109

Professor A. Roshko
California Institute of Technology
Pasadena, California 91109

Professor T.Y. Wu
Department of Engineering
California Institute of Technology
Pasadena, California 91109

Director
Office of Naval Research Branch Office
1030 E. Green Street
Pasadena, California 91101

Naval Ship Engineering Center
Philadelphia Division
Technical Library
Philadelphia, Pennsylvania 19112

Technical Library
Philadelphia Naval Shipyard
Philadelphia, Pennsylvania 19112

Professor R.C. Mac Camy
Department of Mathematics
Carnegie Institute of Technology
Pittsburgh, Pennsylvania 15213

Dr. Paul Kaplan
Oceanics, Inc.
Plainview, Long Island, New York 11803

Technical Library
Naval Missile Center
Point Mugu, California 93441

Technical Library
Naval Civil Engineering Laboratory
Port Hueneme, California 93041

Commander
Portsmouth Naval Shipyard
Portsmouth, New Hampshire 03801

Commander
Norfolk Naval Shipyard
Portsmouth, Virginia 23709

Professor F.E. Bisshopp
Division of Engineering
Brown University
Providence, Rhode Island 02912

Dr. William A. Gross, Vice President
Ampex Corporation
401 Broadway
Redwood City, California 94063

Dr. H.N. Abramson
Southwest Research Institute
8500 Culebra Road
San Antonio, Texas 78228

Editor
Applied Mechanics Review
Southwest Research Institute
8500 Culebra Road
San Antonio, Texas 78206

Office of Naval Research
San Francisco Area Office
50 Fell Street
San Francisco, California 94102

Library
Pearl Harbor Naval Shipyard
Box 400
FPO San Francisco, California 96610

Technical Library
Hunters Point Naval Shipyard
San Francisco, California 94135

Librarian
Naval Ordnance Laboratory
White Oak
Silver Spring, Maryland 20910

Fenton Kennedy Document Library
The Johns Hopkins University
Applied Physics Laboratory
8621 Georgia Avenue
Silver Spring, Maryland 20910

Professor E.Y. Hsu
Department of Civil Engineering
Stanford University
Stanford, California 94305

Dr. Byrne Perry
Department of Civil Engineering
Stanford University
Stanford, California 94305

Dr. R.L. Street
Department of Civil Engineering
Stanford University
Stanford, California 94305

Professor Milton Van Dyke
Department of Aeronautical Engineering
Stanford University
Stanford, California 94305

Professor R.C. Di Prima
Department of Mathematics
Rensselaer Polytechnic Institute
Troy, New York 12180

Professor J. Lumley
Ordnance Research Laboratory
Pennsylvania State University
University Park, Pennsylvania 16801

Dr. M. Sevik
Ordnance Research Laboratory
Pennsylvania State University
University Park, Pennsylvania 16801

Dr. J.M. Robertson
Department of Theoretical and Applied Mechanics
University of Illinois
Urbana, Illinois 61803

Technical Library
Mare Island Naval Shipyard
Vallejo, California 94592

Code 438
Office of Naval Research
Department of the Navy
Arlington, Virginia 22217 (3)

Code 461
Office of Naval Research
Department of the Navy
Arlington, Virginia 22217

Code 463
Office of Naval Research
Department of the Navy
Arlington, Virginia 22217

Code 472
Office of Naval Research
Department of the Navy
Arlington, Virginia 22217

Code 468
Office of Naval Research
Department of the Navy
Arlington, Virginia 22217

Code 473
Office of Naval Research
Department of the Navy
Arlington, Virginia 22217

Code 481
Office of Naval Research
Department of the Navy
Arlington, Virginia 22217

Code 2627
Naval Research Laboratory
Washington, D.C. 20390 (6)

Library, Code 2620 (ONRL)
Naval Research Laboratory
Washington, D.C. 20390 (6)

Code 6170
Naval Research Laboratory
Washington, D.C. 20390

Code 4000
Director of Research
Naval Research Laboratory
Washington, D.C. 20390

Code 8030 (Maury Center)
Naval Research Laboratory
Washington, D.C. 20390

Code 8040
Naval Research Laboratory
Washington, D.C. 20390

Code 031
Naval Ship Systems Command
Washington, D.C. 20390

Code 0341
Naval Ship Systems Command
Washington, D.C. 20390

Code 03412B (L. Benen)
Naval Ship Systems Command
Washington, D.C. 20390

Code 03412 (J. Schuler)
Naval Ship Systems Command
Washington, D.C. 20390

Code 2052
Naval Ship Systems Command
Washington, D. C. 20390

Code 6034
Naval Ship Engineering Center
Center Building
Prince George's Center
Hyattsville, Maryland 20782

Code 6110
Naval Ship Engineering Center
Center Building
Prince George's Center
Hyattsville, Maryland 20782

Code 6113
Naval Ship Engineering Center
Center Building
Prince George's Center
Hyattsville, Maryland 20782

Code 6114
Naval Ship Engineering Center
Center Building
Prince George's Center
Hyattsville, Maryland 20782

Code 6120E
Naval Ship Engineering Center
Center Building
Prince George's Center
Hyattsville, Maryland 20782

Code 6136
Naval Ship Engineering Center
Center Building
Prince George's Center
Hyattsville, Maryland 20782

Dr. A. Powell
Code 01
Naval Ship Research and Development Center
Washington, D.C. 20034

Mr. W.M. Ellsworth
Code 0H50
Naval Ship Research and Development Center
Washington, D.C. 20034

Central Library
Code L42
Naval Ship Research and Development Center
Washington, D.C. 20034

Dr. W.E. Cummins
Code 500
Naval Ship Research and Development Center
Washington, D.C. 20034

Mr. S.F. Crump
Code 513
Naval Ship Research and Development Center
Washington, D.C. 20034

Mr. R. Wermter
Code 520
Naval Ship Research and Development Center
Washington, D.C. 20034

Dr. P. Pien
Code 521
Naval Ship Research and Development Center
Washington, D.C. 20034

Dr. W.B. Morgan
Code 540
Naval Ship Research and Development Center
Washington, D.C. 20034

Mr. P. Granville
Code 541
Naval Ship Research and Development Center
Washington, D.C. 20034

Mr. J.B. Hadler
Code 560
Naval Ship Research and Development Center
Washington, D.C. 20034

Dr. H.R. Chaplin
Code 600
Naval Ship Research and Development Center
Washington, D.C. 20034

Mr. G.H. Gleissner
Code 800
Naval Ship Research and Development Center
Washington, D.C. 20034

Dr. M. Strasberg
Code 901
Naval Ship Research and Development Center
Washington, D.C. 20034

Mr. J. McCarthy
Code 552
Naval Ship Research and Development Center
Washington, D.C. 20034

Code 03
Naval Air Systems Command
Washington, D.C. 20360

AIR 5301
Naval Air Systems Command
Department of the Navy
Washington, D.C. 20360

Code ORD 03
Naval Ordnance Systems Command
Washington, D.C. 20360

Code ORD 035
Naval Ordnance Systems Command
Washington, D.C. 20360

Code ORD 05413
Naval Ordnance Systems Command
Washington, D.C. 20360

Code ORD 9132
Naval Ordnance Systems Command
Washington, D.C. 20360

Oceanographer of the Navy
Washington, D.C. 20390

Commander
Naval Oceanographic Office
Washington, D.C. 20390

Chief Scientist (CNM PM-1)
Strategic Systems Project Office
Department of the Navy
Washington, D.C. 20360

Technical Division (CNM PM 11-20)
Deep Submergence Systems Project Office
Department of the Navy
Washington, D.C. 20360

Dr. A.L. Slafkosky
Scientific Advisor
Commandant of the Marine Corps (Code AX)
Washington, D.C. 20380

Librarian Station 5-2
Coast Guard Headquarters
NASSIF Building
400 7th Street, S.W.
Washington, D.C. 20591

Office of Research and Development
Maritime Administration
441 G. Street, N.W.
Washington, D.C. 20235

Division of Ship Design
Maritime Administration
441 G. Street, N.W.
Washington, D.C. 20235

National Science Foundation
Engineering Division
1800 G. Street, N.W.
Washington, D.C. 20550

Dr. G. Kulin
National Bureau of Standards
Washington, D.C. 20234

Science & Technology Division
Library of Congress
Washington, D.C. 20540

Chief of Research & Development
Office of Chief of Staff
Department of the Army
The Pentagon, Washington, D.C. 20310

Professor A. Thiruvengadam
Department of Mechanical Engineering
The Catholic University of America
Washington, D.C. 20017

Professor G. Birkhoff
Department of Mathematics
Harvard University
Cambridge, Massachusetts 02138

AIR 604
Naval Air Systems Command
Department of the Navy
Washington, D.C. 20360

Dr. A.S. Iberall, President
General Technical Services, Inc.
451 Penn Street
Yeadon, Pennsylvania 19050

Professor J.F. Kennedy, Director
Iowa Institute of Hydraulic Research
State University of Iowa
Iowa City, Iowa 52240

Professor L. Landweber
Iowa Institute of Hydraulic Research
State University of Iowa
Iowa City, Iowa 52240

Dr. Lee Segel
Department of Mathematics
Rensselaer Polytechnic Institute
Troy, New York 12180

Code 6101E
Naval Ship Engineering Center
Center Building
Prince George's Center
Hyattsville, Maryland 20782